

University of Southern Queensland
Faculty of Engineering and Surveying

**The Effect of Reinforcement Ratio on the
Compressive Behaviour of Glass Fibre Reinforced
Polymer (GFRP) reinforced Concrete Columns with
Hollow Composite Reinforcing Section (HCRS)**

Final Dissertation submitted by
Michael Ng

In fulfilment of ENG4111 Research Project 1 and
ENG41112 Research Project 2 towards the degree of
Bachelor of Civil Engineering

Submitted: 17 October 2019

Supervisors: Dr. Allan Manalo; Omar AlAjarmeh

Project Title

The Effect of Reinforcement Ratio on the Compressive Behaviour of Glass Fibre Reinforced Polymer (GFRP) reinforced Concrete Columns with Hollow Composite Reinforcing Section (HCRS)

Abstract

Steel reinforcing bars are the most common and effective reinforcement for concrete structures. However, steel corrosion in concrete has been a significant problem in some environments as concrete deterioration reduces the life of structures and involves high repair costs as a result; most of all, it can endanger the integrity of the structures and affect other elements of construction.

In recent years, fibre reinforced polymer has been used as an alternative reinforcement, offering a number of advantages over steel especially when used in marine and other harsh environments. The most common type of fibre polymer material is glass fibre reinforced polymers (GFRP) as they are cost effective and corrosion resistant. In some standards, however, suggested that using GFRP bars as longitudinal reinforcement is not recommended due to its low compressive strength and few researches have been conducted to examine its credentials.

The objective of this study is to investigate the stress/strain strength and the failure mode of the concrete columns with different reinforcement ratios. A total of three hollow concrete columns reinforced longitudinally with GFRP bars with different reinforcement ratios (1.74%, 2.6% and 3.47%) and hollow composite reinforcing system (HCRS) were prepared. The different reinforcement ratios were achieved by placing different number of 15.9mm diameter GFRP bars (4, 6 and 8 bars respectively).

Hollow concrete columns were tested in this study. Hollow columns are considered to be a structurally efficient construction system due to the cost saving by decreased section area. A hollow composite reinforcing system (HCRS) was placed in each column to provide reinforcement in both longitudinal and transverse directions. HCRS are made by GFRP tubes with four studs attached to the full length of the hollow section to enhance the bonding between concrete and the HCRS.

To date, limited researches have been conducted on the concrete columns reinforced with GFRP combined with HCRS. Therefore, this study focused on the compressive behaviour of this innovative reinforcing system under concentric axial load.

ENG4111 & ENG4112 Research Project

Limitations of Use

The Council of the University of Southern Queensland, its Faculty of Health, Engineering and Sciences, and the staff of the University of Southern Queensland, do not accept any responsibility for the truth, accuracy or completeness of material contained within or associated with this dissertation.

Persons using all or any part of this material do so at their own risk, and not at the risk of the Council of the University of Southern Queensland, its Faculty of Health, Engineering and Sciences or the staff of the University of Southern Queensland.


This dissertation reports an educational exercise and has no purpose or validity beyond this exercise. The sole purpose of the course pair entitled “Research Project” is to contribute to the overall education within the student’s chosen degree program. This document, the associated hardware, software, drawings, and any other material set out in the associated appendices should not be used for any other purpose: if they are so used, it is entirely at the risk of the user.

Certification of Dissertation

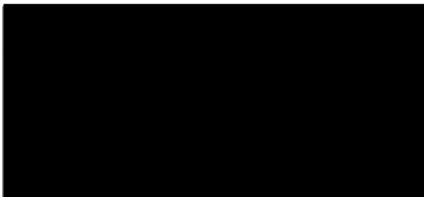
I certify that the ideas, designs and experimental work, results, analyses and conclusions set out in this dissertation are entirely my own effort, except where otherwise indicated and acknowledged.

I further certify that the work is original and has not been previously submitted for assessment in any other course or institution, except where specifically stated.

Student Name: Michael Ng

Student Number: 

Signature:



Date: 17th October 2019

Acknowledgments

Foremost, I would like to express my appreciation over to my supervisors, Dr. Allan Manalo, and Omar AlAjarmeh for giving me the opportunity to work on this research and providing support throughout this year. It was a great privilege and honour to study under their guidance. I would also like to thank the Z block laboratory staff for assisting me to use the equipment.

I am grateful to Inconmat V-ROD Australia for providing the GFRP bars, spirals and the HCRS.

Last but not least, I would like to thank my family, my wife, Miyuki and my daughters, Kaye and Emi, for their understanding and support throughout my study.

TABLE OF CONTENTS

| | |
|---|----|
| Project Title | 2 |
| Abstract | 2 |
| Acknowledgments | 5 |
| | |
| 1. Introduction | |
| 1.1 Background | 8 |
| 1.2 Research objectives | 9 |
| 1.3 Research approach | 9 |
| | |
| 2. Literature review | |
| 2.1 Introduction | 13 |
| 2.2 Properties of GFRP bars and spirals | 15 |
| 2.3 Benefits and limitations to GFRP bars and spirals | 16 |
| 2.4 Properties of HCRS | 17 |
| 2.5 Benefits and limitations to HCRS | 18 |
| 2.6 Conclusion | 19 |
| | |
| 3. Project methodology | |
| 3.1 Project materials | |
| 3.1.1 Specimen parameters | 20 |
| 3.1.2 Materials for the reinforcement | 22 |
| 3.1.3 Concrete grading and preparation | 22 |
| 3.1.4 Summary of the key phases for the laboratory test | 25 |
| 3.2 Test set up, procedures and data collection | 28 |
| 3.3 Risk assessment | 29 |

| | |
|--|----|
| 4. Results and discussion | |
| 4.1 Failure mode | 31 |
| 4.2 Load-deformation behaviour | |
| 4.2.1 Load-deformation behaviour of Test columns | 37 |
| 4.2.2 Load-deformation behaviour of Controlled columns | 39 |
| 4.3 Strain behaviour of the GFRP bars and spirals | |
| 4.3.1 Strain behaviour of the GFRP bars and spirals for Test columns | 41 |
| 4.3.2 Strain behaviour of the GFRP bars and spirals for Controlled columns | 42 |
| 4.4 Strain behaviour of HCRS and the concrete | |
| 4.4.1 Strain behaviour of HCRS for all hollow concrete columns | 43 |
| 4.4.2 Strain behaviour of the concrete for all hollow concrete columns | 44 |
| 4.5 Influence of the number of GFRP bars | 45 |
| 4.6 Influence of HCRS | 46 |
| | |
| 5. Theoretical analysis of column behaviour | |
| 5.1 Crushing strain and axial stress of the GFRP bars | 48 |
| 5.2 Axial-load capacity (1 st peak load) | 51 |
| 5.3 Axial-load capacity (2 nd peak load) | 52 |
| | |
| 6. Conclusions | 57 |
| | |
| 7. References | 58 |
| | |
| Appendix A: Project Specification | 59 |
| Appendix B: Project Plan | 60 |
| Appendix C: Laboratory Induction Checklist | 61 |

1. Introduction

1.1 Background

A reinforced concrete column is a structural member designed to support the weight of the structure above through compression. Even though columns are mostly subjected to compressive loads, there are always lateral forces due to wind or seismic loads. Therefore, it is important to design a column with steel reinforcement to provide much needed tensile strength and ductility for the flexural forces. Steel reinforcements would also resist cracking which can occur due to shrinkage.

Corrosion of steel reinforcing bars in concrete is a major problem which causes deterioration in concrete. When steel corrodes, the rusting generates greater volume and this expansion creates additional tensile stresses inside the concrete, causing cracking and spalling as a result. To address this problem, scientists and engineers have spent a significant amount of time in researches to find alternative materials that replace the conventional steel reinforcing bars.

As a result, fibre reinforced polymer (FRP) bars have become more widespread as an alternative to conventional steel reinforcement for concrete structures. FRP bars use composite materials to strengthen concrete structures and they are commonly made with glass, carbon or aramid. FRPs are characterised by their resistance to corrosion, and have many other advantages; they are lightweight and nonmagnetic, and have high tensile strength and low thermal and electrical conductivity. On the other hand, FRP bars are known to have low transverse strength, low modulus of elasticity and no yielding before failure.

The most common type of fibre polymer material is glass fibre reinforced polymers. The use of GFRP bars as concrete reinforcement is a competitive option not only because they are cost effective, but also corrosion resistant and have high electrical/heat insulating properties. For such characteristics, they are suitable for structures that operate in aggressive environments, such as in coastal areas or chemical plants. However, GFRP bars are relatively weak in compression due to the low modulus of elasticity, while having a higher tensile strength (approximately 1200MPa) compared to conventional steel rebar (500MPa).

In this study, hollow composite reinforcing section HCRS will be introduced as a second reinforcement in the hollow concrete columns. Each HCRS contains 4 x 25mm long studs to create better bonding and interlocking with the concrete column.

HCRS uses high strength glass fibre reinforced polymer which can significantly enhance the confinement of the concrete core and ductility. The placement of longitudinal HCRS at the centre of the column creates high section moment of inertia and flexural capacity. A hollow column will also reduce the volume of concrete required for construction; hence reduce the construction costs and greenhouse gas emissions in the environment.

1.2 Research objectives

Hollow concrete columns have higher structural performance compared to solid concrete columns due to the high strength-to-weight ratios. A number of researchers found that the overall behaviour of hollow reinforced concrete columns largely depends on the longitudinal reinforcement ratio and the lateral reinforcement details. Since the corrosion of steel reinforcement is a major problem with concrete columns, fibre-reinforced-polymer has become an effective alternative to steel reinforcement. The use of Glass fibre reinforced polymer (GFRP) bars is common because of its competitive cost and close modulus of elasticity. In this study, 15.9mm diameter GFRP bars (Figure 1) and 3mm GFRP spirals (Figure 2) were used with 65mm diameter x 5mm thick hollow composite reinforcing system (HCRS) installed longitudinally in the centre of the concrete columns.

Glass fibre reinforced polymer bars are high in tensile strength but low in transverse strength. This project focuses on the behaviour of this hybrid reinforcing system - GFRP bars/spirals and HCRS under compressive loads through laboratory testing and analysis. Research objectives of this study are:

- Investigating the effect of reinforcement ratio by experimentally increasing the number of GFRP bars;
- Theoretical evaluation and predication of failure load for hollow concrete columns reinforced with GFRP bars and HCRS;
- Investigating the strength and strain capacities of the concrete column reinforced and confined by GFRP bars and HCRS; and
- Investigating the contribution of GFRP spiral in order to eliminate longitudinal bar buckling.

1.3 Research approach

In this study, a total of six concrete columns 250mm in diameter and 1m height were casted and tested. Specimens #2, #4 and #5 were reinforced longitudinally with GFRP bars/spiral and HCRS (refer to Table 1). 6, 4 and 8 pieces of 15.9mm diameter GFRP bars were inserted into the columns - specimens #2, #4 and #5 respectively. This provided the reinforcement ratios (μ) of 2.6% (#2), 1.74% (#4) and 3.47% (#5) (refer to Table 2). The range of 1% to 4% reinforcement ratio is recommended by AS3600 for steel reinforced concrete columns.

The results of specimens #2, #4 and #5 are compared to #6, #7 and #8 – the controlled specimens. As indicated in table 1, specimen #6 was reinforced with 6 x 15.9mm GFRP bars with 3mm GFRP spiral and a 65mm diameter PVC pipe installed longitudinally in the centre of the column. Specimens #7 was reinforced with HCRS and 3mm GFRP spiral, while specimen #8 being reinforced with GFRP spiral only (with PVC placed in the centre to create the void).



Figure 1: Sand-coated GFRP Bars (15.9mm nominal diameter)



Figure 2: Sand-coated GFRP Spirals (9.5mm nominal diameter)



Figure 3: Hollow composite reinforcing system HCERS

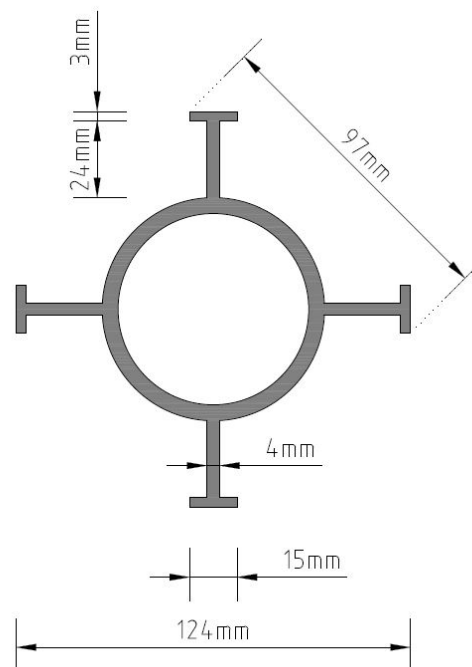


Figure 4: Schematic diagram of HCERS

| Specimen Number # | Type of longitudinal reinforcement | Number of longitudinal bars | Bar diameter (mm) | Diameter of GFRP spirals (mm) | Spacing of spirals (mm) | Compressive strength of concrete (MPa) | Remarks |
|-------------------|------------------------------------|-----------------------------|-------------------|-------------------------------|-------------------------|--|---------------------|
| 2 | GFRP / HCRS | 6 | 15.9 | 3 | 50 | 35 | Test specimen |
| 4 | GFRP / HCRS | 4 | 15.9 | 3 | 50 | 35 | Test specimen |
| 5 | GFRP / HCRS | 8 | 15.9 | 3 | 50 | 35 | Test specimen |
| 6 | GFRP | 6 | 15.9 | 3 | 50 | 35 | Controlled specimen |
| 7 | HCRS | - | - | 3 | 50 | 35 | Controlled specimen |
| 8 | - | - | - | 3 | 50 | 35 | Controlled specimen |

Table 1: Summary of the test specimens

| Specimen Number # | Number of Bars | Bar Diameter (mm) | Total Reinforcement Area (mm ²) | Reinforcement Ratio, (%) |
|-------------------|----------------|-------------------|---|--------------------------|
| 2 | 6 | 15.9 | 1191.3 | 2.6 |
| 4 | 4 | 15.9 | 794.2 | 1.74 |
| 5 | 8 | 15.9 | 1588.5 | 3.47 |

Table 2: Details of the Test column specimens

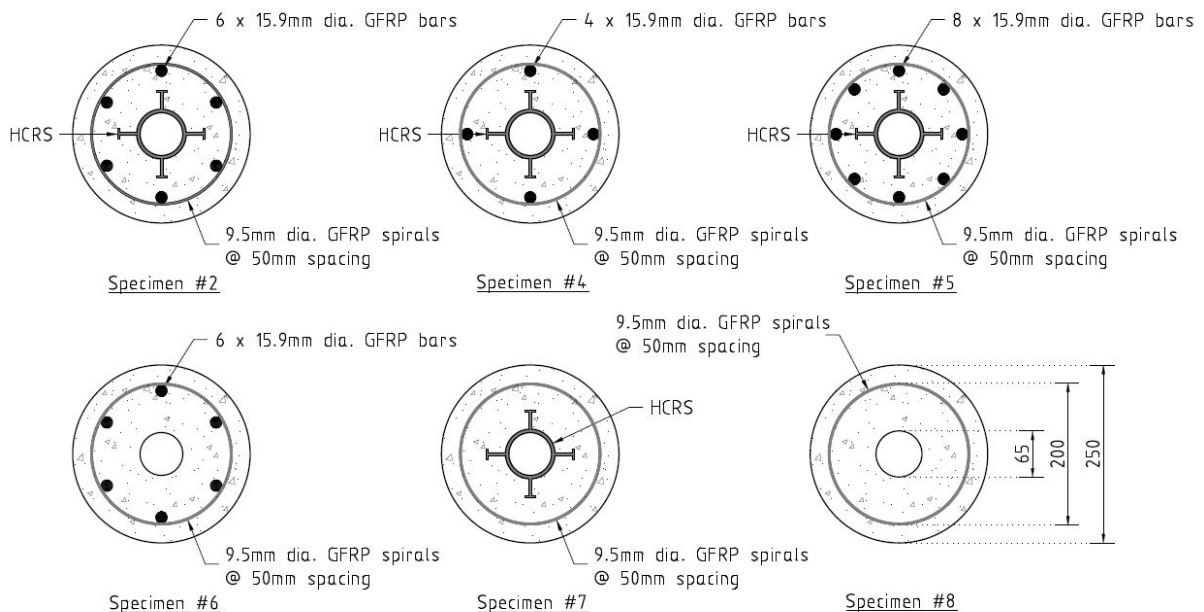


Figure 5: Column cross sections
 (#2, #4, #5 – Test specimen & #6, #7, #8 – Controlled specimen)

2. Literature review

2.1 Introduction

Deterioration of infrastructure has been well documented in most countries for the last few decades. In recent years, the use of glass fibre reinforced polymer (GFRP) bars are becoming popular as the main reinforcement for concrete structures. It has been widely accepted as a solution to overcome the problem of steel corrosion. GFRP is also non-magnetic and lightweight with low thermal and electrical conductivity. This makes the GFRP bars well suited for use in corrosive environments, as well as places like hospitals due to its non-magnetic nature. GFRP material has a very long life span compared to steel and provides easy workability because of the lightweight.

A limited number of studies, however, have been conducted to evaluate the mechanical properties of GFRP bars under compression. The compressive strength of GFRP bars is relatively low compared to their tensile strength. Various factors, such as the fibre type, fibre volume ratio, length to diameter ratio, boundary conditions and the manufacturing process may affect the compressive strength of GFRP bars.

As an earlier research suggests (Chaallal, O; Benmokrane, B; 1993), the strength and stiffness of GFRP bars in compression ranges between 30% and 70% compared to their tension values. Experiments from Kobayashi and Fujisaki (1995) tested various fibre materials (i.e. aramid, carbon and glass) as reinforcing bars in compression. The results showed that the compressive strengths of aramid, carbon and glass fibre were 10%, 30% and 30% respectively to their corresponding tensile strengths. Therefore, it was concluded that the ultimate compressive strength of GFRP bar is approximately 30% of its corresponding tensile strength.

A series of studies conducted by Tobbi et al (2012) indicated that concrete columns with GFRP bars could be used in compression members, provided that there is sufficient confinement in the GFRP spirals to eliminate bar buckling. GFRP spirals are high in tensile strength and will increase the ultimate capacity of longitudinal bars; hence delaying buckling.

In this study, a second reinforcement – hollow composite reinforcing system (HCRS) was introduced to provide additional core confinement, so that it increases the tensile and flexural strengths to overcome the low compressive strength of GFRP in the concrete column. HCRS is made of high strength glass fibre reinforced polymer that is light weight and high stiffness, contributing to the improvement of the strength-to-weight ratio of the concrete column.

In recent years, high strength fibre reinforced polymer composite materials have been used in construction industry, especially in seismic regions. By placing the HCRS in the centre of the concrete column, it increases the compressive strength and ductility. In order to create a better bond with the concrete, four studs will be attached to the full length of the hollow section; thereby enhancing the flexural strength and prevents buckling.

Since the use of fibre reinforced polymer composites as the main longitudinal reinforcement is relatively new, theoretical work in this area is limited. To date, only a few of experimental researches have been conducted on the compressive behaviour of concrete columns reinforced with GFRP bars/spirals combined with hollow composite reinforcing system. This paper reports the test results of stress/strain strength and the failure mode, as well as the effect of numbers of GFRP bars on each RC column specimens. Furthermore, this paper will investigate the feasibility and benefits of the proposed composite column.

The literature review was conducted by using Google Scholar with keywords/phases below:

Concrete column, glass fibre-reinforced polymer bars (GFRP), hollow composite reinforcing system (HCRS), high strength polymer fibre composites, compressive strength, flexural strength, axial load, ductility, buckling.

2.2 Properties of GFRP reinforcement

GFRP bars and spirals were used to reinforce the hollow RC column specimens in the longitudinal and traverse directions. All GFRP bars/spirals were sand-coated to enhance bonding between the reinforcement and concrete. The nominal diameters of GFRP bars and spirals were 15.9mm and 9.5mm respectively. The GFRP reinforcement was manufactured by pultrusion with glass fibres impregnated in a thermosetting vinyl ester resin, additives and fillers. The mechanical properties of GFRP bars reported by Benmokrane et al. (2017) are listed in Table 3 below.

| Properties | Test Method | Number of Samples Tested | Values |
|---|----------------------|--------------------------|--------|
| Nominal bar diameter (mm) | CSA S806, Annex A | 9 | 15.9 |
| Nominal bar area (mm ²) | CSA S806, Annex A | 9 | 198.5 |
| Ultimate tensile strength, f_u (Mpa) | ASTM D7205/D7205M-06 | 6 | 1237.4 |
| Modulus of Elasticity, E_{GFRP} (Gpa) | ASTM D7205/D7205M-06 | 6 | 60.5 |
| Ultimate strain, E_u (%) | ASTM D7205/D7205M-06 | 6 | 2.1 |

Table 3: Mechanical properties of GFRP bars (15.9mm nominal diameter)
(Source: Benmokrane et al. 2017)

2.3 Benefits and limitations of GFRP reinforcement

Benefits of GFRP reinforcement

GFRP reinforcement offer many advantages over conventional steel bars. Some of these benefits are as follows:

- Corrosion resistance – GFRP is not made from steel, therefore it does not react with salt and chemical products. It makes GFRP as an ideal reinforcing material for concrete when exposed to corrosive environments, for example, floating structures, roads and carparks, chemical plants.
- Superior tensile strength – GFRP rebar is made by pultrusion process with glass fibres impregnated in a thermosetting vinyl ester resin, additives and fillers. It offers a tensile strength up to twice as much as normal structural steel. In this study, the ultimate tensile of 15.9mm diameter GFRP bar is approximately 1200MPa, whereas it is 500MPa for conventional steel rebar.
- Thermal insulation and expansion – Due to its 80% of silica content, GFRP rebar has high thermal insulation and low thermal expansion.
- Electric and magnetic neutrality – GFRP does not contain any metal, therefore it does not interfere with the magnetic fields caused by the electronic equipment.
- Lightweight – According to the studies by Benmokrane et al. (2006, 2007) GFRP reinforcement has a quarter of the weight of steel. This makes significant savings in transportation and installation.

Limitations of GFRP bars and spirals

Previous researches indicated that the strength and modulus of GFRP reinforcement in tension were higher than in compression. Chaallal and Benmokrane (1993) investigated the compressive behaviour of GFRP bars and found that the compressive strength was 77% of the tensile strength. Kobayashi and Fujisaki (1995) tested GFRP bars embedded inside the concrete prisms, and the results showed that the compressive strengths of GFRP bars were around 30% to 40% of tensile strengths. Similarly, a recent study by Tobbi et al. (2012) has tested square RC columns with GFRP bars and spirals. In its findings, the compressive strength of GFRP bars was 35% of its tensile strength. There is a consensus that the compressive strength of GFRP reinforcement is lower than the tensile strength. According to previous findings, GFRP bars in compression varied between 30% to 70% to tension. In this study, the test results of Tobbi et al. has been adopted and the compressive strength of GFRP bars would be taken as 35% of the ultimate tensile capacity.

GFRP bar has low compressive strength compared to its tensile counterpart due to its fibre micro-buckling attributable to the anisotropic and nonhomogeneous nature of the FRP material (Afifi et al. 2013). As a result, some design guidelines such as ACI440.1R (ACI Committee 4402006) do not recommend the use of GFRP bars as longitudinal reinforcement in compression members.

2.4 Properties of HCRS

The confining pressure of the HCRS subjects the core concrete to a triaxial state of stress. According to a study conducted by Becque et al. (2003), HCRS has anisotropic material properties because it is made by filament wound tube using unidirectional E-glass fibres and a polyester resin. Therefore, the elastic modulus in the longitudinal direction is different to the elastic modulus in the hoop direction. The properties of the hollow HCRS are listed in Table 4 below.

| Properties | Test Standard | Values |
|-----------------------------------|----------------------|--------|
| Density (kg/m ³) | ASTM D792 | 1926.5 |
| Fibre content by weight (%) | ASTM D2584 | 73.20% |
| Glass transition temperature (°C) | ASTM E1356 | 81.4 |
| Axial compression (MPa) | ASTM D695 | 120.4 |
| Transverse compression (MPa) | ISO 14125 (1998) | 8.8 |
| Transverse shear strength (MPa) | ASTM D2344/D2344M-13 | 7.5 |
| Interlaminar shear strength (MPa) | ASTM D4475 | 22.1 |
| Flexural strength (MPa) | ASTM D790 | 201.1 |
| Flexural modulus (GPa) | ASTM D790 | 42.1 |

Table 4: Physical and mechanical properties of HCRS
(Source: Centre of Future Materials, University of Southern Queensland)

2.5 Benefits and limitations of HCRS

Benefits of HCRS reinforcement

The use of HCRS provides inner radial confinement for the hollow concrete columns. Similarly, the concrete core prevents HCRS to buckle outwards. Jurgen Becque et al. (2003) found that the load carrying capacity of the composite column was greater than the sum of the capacity of unconfined concrete and the capacity of HCRS. HCRS also acts as a uniform longitudinal reinforcement located at the core of the column to resist moments, improving the stiffness and ductility of the hollow column.

Furthermore, HCRS is made by glass fibre polymer which provides a non-corrosive reinforcement for the RC column. HCRS is light weight and easy to handle compared to steel tube. Amir Z. Fam et al. (2002) has conducted a strength-to-weight research on hollow RC columns and found that a hollow column with 9 % less weight than a solid counterpart (same height and diameter as a hollow column) had 35 % higher strength-to-weight ratio.

Limitations of HCRS reinforcement

The maximum load-carrying capacity of hollow column is less than a solid column due to its central void. The strength of HCRS generally depends on the alignment of the fibre. For example, with a GFRP tube made by pultrusion with all fibres in the axial direction, the tensile strength is strong in longitudinal direction but weak in hoop direction. Alternatively, a filament wound GFRP tube with unidirectional fibres would distribute the strengths between the longitudinal and hoop directions depending on the angles of the fibres. Consequently, the alignment of fibres and the non-homogeneous nature of GFRP tube can make the properties of HCRS vary greatly in different directions.

2.6 Conclusion

Some design guidelines do not recommend the use of GFRP bars as longitudinal reinforcement in compression member due to its low compressive strength. However, confined concrete behaves differently to unconfined concrete. In this study, an innovative hybrid reinforcement system– GFRP bars/spirals with HCRS, was introduced and the core of RC column specimens were confined by the GFRP spirals and HCRS. This report will investigate the compressive behaviour and evaluate the strength and strain capacities of RC columns reinforced with hybrid reinforcement system.

3. Project methodology

3.1 Project materials

3.1.1 Specimen parameters

The objective of experimental work was to investigate the effect of number of GFRP bars on the behaviour of concrete columns with HCRS. It involved the testing of six RC columns - 250mm in diameter and 1m height under concentric axial load. All specimens had a 65mm hollow core. Specimens #2, #4 and #5 were reinforced longitudinally with GFRP bars/spirals and HCRS. The results of these specimens were compared to the controlled specimens, #6, #7 and #8. A summary of these six hollow concrete columns is shown below (Figure 6).

Specimen #2 “T”: Reinforced longitudinally 6 x 15.9mm dia. GFRP bars with 9.5mm dia. spirals (50mm spacing) and HCRS.

Specimen #4 “T”: Reinforced longitudinally 4 x 15.9mm dia. GFRP bars with 9.5mm dia. spirals (50mm spacing) and HCRS.

Specimen #5 ”T”: Reinforced longitudinally 8 x 15.9mm dia. GFRP bars with 9.5mm dia. spirals (50mm spacing) and HCRS.

Specimen #6 “C”: Reinforced longitudinally 6 x 15.9mm dia. GFRP bars with 9.5mm dia. spirals (50mm spacing)

Specimen #7 “C”: Reinforced with 9.5mm dia. spirals (50mm spacing) and HCRS.

Specimen #8 “C”: Reinforced with 9.5mm dia. spirals (50mm spacing)

Note: Specimen #2, #4 and #5 were test specimens (denoted “T”).
Specimen #6, #7 and #8 were controlled specimens (denoted “C”).

The reinforcement ratio (ρ) for specimens #2, #4 and #5 were as follows:

Specimen #2 “T”: 2.6% (6 x 15.9mm dia GFRP bars)

Specimen #4 “T”: 1.74% (4 x 15.9mm dia GFRP bars)

Specimen #5 “T”: 3.47% (8 x 15.9mm dia GFRP bars)

The reinforcement ratio (ρ) for the 9.5mm diameter spirals was 1.53%



(a)



(b)

Figure 6: Overview of the assembled cages: (Left to Right) Specimens #8, #4, #2 and #5

3.1.2 Materials for the reinforcement

The GFRP bars and spirals were manufactured by pultrusion with glass fibres impregnated in a thermosetting vinyl ester resin, additives and fillers. GFRP reinforcement had a sand coated surface to enhance the bonding between the bars and the concrete. The longitudinal bars had a nominal diameter of 15.9mm and the spirals were 3mm in diameter. The tensile strength of the GRPS reinforcement was 1200MPa and the Modulus of Elasticity was 60.5GPa.

The hollow Composite Reinforcing System HCRS was made of high strength glass fibre reinforced polymer. It was one metre long and 70mm outside diameter with 5mm wall thickness. There were four studs (27mm long) attached to the full length of the hollow section to enhance the bonding/interlocking between concrete and the hollow section. The axial compression strength of the hollow section was 120.4MPa. Furthermore, HCRS has good thermal stability and chemical resistance; ideal to be used as concrete reinforcement.

3.1.3 Concrete grading and preparation

A compressive strength at 28 days of nominal 35MPa concrete, with a slump of 200mm and maximum aggregate size of 10mm, was used in this study. All six columns were casted at the same time using one concrete batch. The batch was taken on cylinder samples and the 28 days compressive strength was recorded. Each column specimen was cured in the laboratory at ambient temperature in order to achieve the predicted maximum compressive strength. No additives were used in any of the specimens.

PVC pipe (250mm dia.) was used as a mould for casting the concrete specimens (Figure 7). The PVC moulds were fixed vertically to the timber formwork (Figure 9) with the reinforcement cages placed into the mould. Concrete spacers (Figure 8) was used to provide minimum of 25mm cover for GFRP bars and spiral. HCRS were centrally placed inside specimens #2, #4, #5 and #7 by using the non-corrosive plastic ties.



(a)



(b)

Figure 7: (a) 250mm dia PVC pipe
(b) Placement of reinforcement cage inside PVC pipe

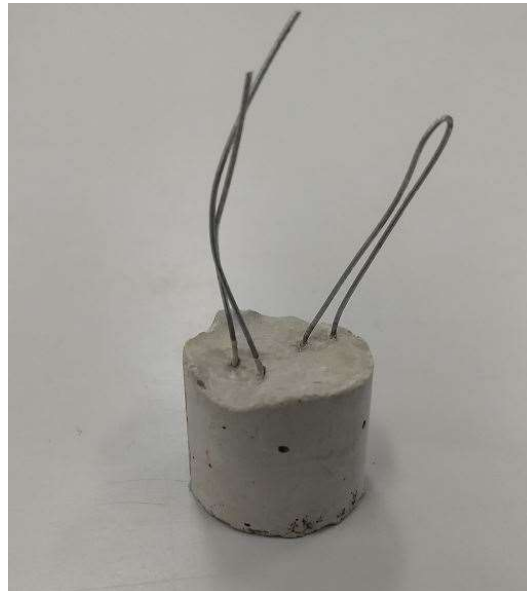


Figure 8: 25mm Concrete spacer



Figure 9: Timber formwork supporting the concrete column specimens

3.1.4 Summary of key phases for the laboratory test

The materials for the RC column specimens were provided by USQ Research Centre, Toowoomba campus. The key phases for the laboratory preparation are stated below.

1. Safety induction program:

Before accessing to the laboratory, students must attend a safety induction class with the laboratory staff, ensuring that the emergency procedures are understood and the laboratory equipment are used correctly. Appropriate personal protective equipment (PPE) must be worn at all times inside the laboratory (Refer appendix C).

2. Preparation of concrete reinforcement:

Students were required to prepare reinforcement cages with GRFP bars and spirals. Reinforcement bars and spirals were tied with non-corrosive plastic cable ties. Students must ensure all the longitudinal bars were evenly located and the spirals were at 50mm spacing. HCRS were located centrally inside the columns for specimens #2, #4, #5 and #7. By predrilling holes at the end of the HCRS studs and using the cable ties, HCRS was secured firmly to the reinforcement cages.

3. Placement of Strain Gauge:

Strain gauges were mounted at the mid height of each column specimen to measure the strain of the longitudinal reinforcement (2 gauges, one on each bar at the opposite location), spiral reinforcement (2 gauges, place each gauge at the opposite location), HCRS (2 gauges, place each gauge at the opposite location) and concrete (2 gauges, place each gauge on the outer surface of the column at the opposite location). Refer figure 10 for the location of the electrical-resistance strain gauges.

The experimental test results of the axial deformations, axial and hoop strains were recorded through the System 5000 data logger. The failure of the concrete columns was carefully observed and video-recorded during the entire loading test.

4. Preparation of concrete pour:

Prior to the concrete placement, PVC moulds with reinforcement cages inside must be supported and secured in a vertical position with the formworks (Figure 11). Concrete was poured into each PVC mould through the chute of the concrete truck. An electric vibrator (Figure 12) was used to ensure the concrete pour was even and free of air bubbles.

During the concrete pour, one-cylinder sample must be taken for each concrete batch. It is important that all concrete batches were tested, reaching the maximum 28 days compressive strength prior to testing.

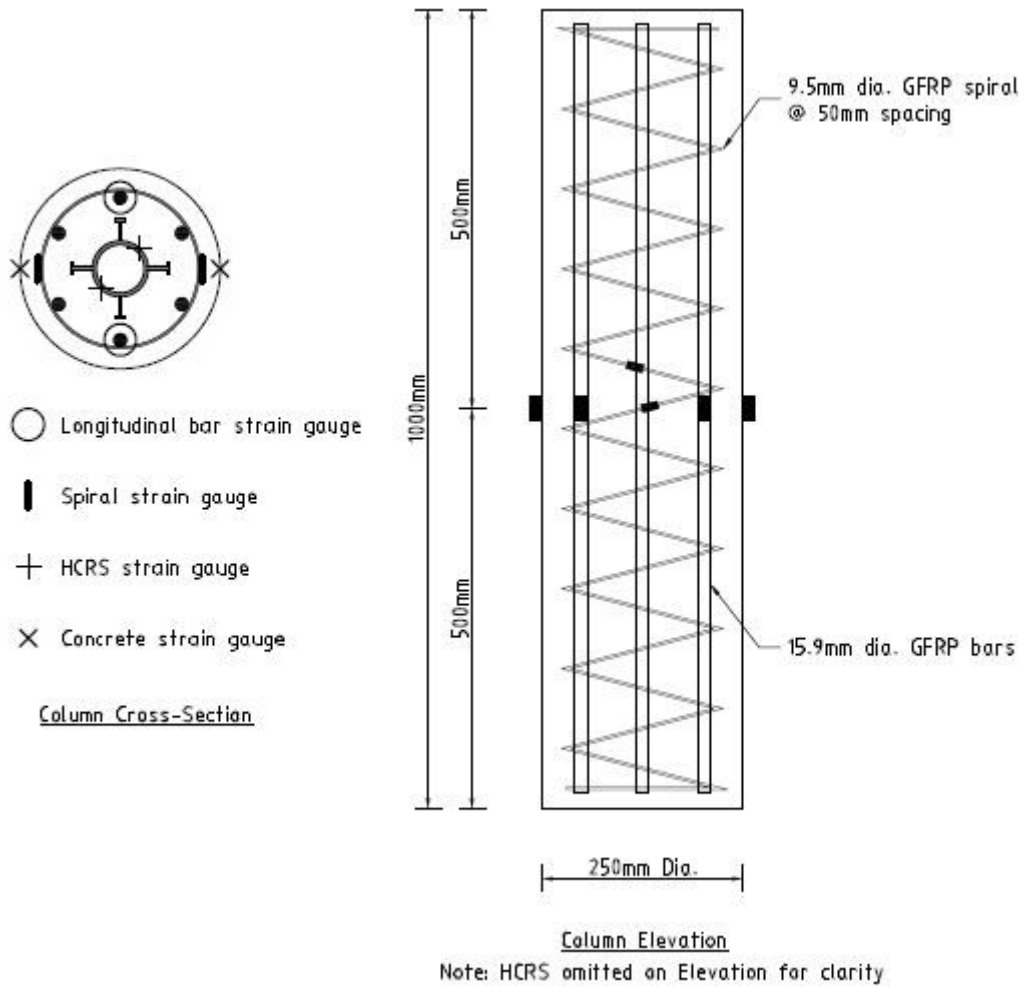


Figure 10: Location of the electrical-resistance strain gauges



Figure 11: Specimens fixed vertically by the timber formwork prior to concrete placement



Figure 12: Electric vibrator used during concrete pour

3.2 Test set up, procedures and data collection

The column specimens were tested under monotonic concentric loading by using a 2000kN hydraulic cylinder with a loading rate of 1.5mm per minute. One steel clamp (50mm in width and 10mm in thickness) was used at the bottom of the specimen for column #4, #5, #6 and #7 to prevent premature cracking and ensure that failure would start at column mid-height (Note: steel clamp not used for #2 and #8). In addition, neoprene rubber pads (3mm thick) were placed at the top and bottom of all the columns for uniform load distribution. Throughout testing, loads, axial deformations and strains were recorded with a System 5000 data logger. Failure propagation was video recorded and observed during entire testing.

3.3 Risk assessment

Risk assessment is a systematic approach to identify and review activities, situations locations and procedures in order to control hazards and manage risks. This process involves a series of steps and actions as follows:

1. Who is involved?
2. Identify hazards by priority.
3. Analyse possible consequences.
4. Assess the risks. Analyse the probability, frequency and severity.
5. Eliminate or remove the risks.
6. Implement risk controls.
7. Review control measures. Redesign and safety audit.

Likelihood and consequences of risks is determined on a scale shown below (Table 5).

| A ssess the likelihood and consequences from the hazards or risks | | | | | |
|--|--|--|---|---|--|
| Likelihood | Consequences | | | | |
| | Insignificant <i>No injury, 0 - low \$ loss</i> | Minor <i>First Aid injury, low - medium \$ loss</i> | Moderate <i>Medical Treatment, medium - high \$ loss</i> | Major <i>Serious injuries, major \$ loss</i> | Catastrophic <i>Death, huge \$ loss</i> |
| Almost Certain <i>is expected to occur at most times</i> | H - 5 | H - 4 | E - 3 | E - 2 | E - 1 |
| Likely <i>will probably occur at most times</i> | M - 6 | H - 5 | H - 4 | E - 3 | E - 2 |
| Possible <i>might occur at some time</i> | L - 7 | M - 6 | H - 5 | E - 4 | E - 3 |
| Unlikely <i>could occur at some time</i> | L - 8 | L - 7 | M - 6 | H - 5 | E - 4 |
| Rare <i>may occur in rare circumstances</i> | L - 9 | L - 8 | M - 7 | H - 6 | E - 5 |

Code: E – Extreme Risk; H – High Risk; M – Moderate risk; L – Low risk

Table 5: Risk matrix used in local government departments

Using a risk methodology table established by the local council, concerns are stated into the likelihood and consequence (Table 6). This indicates the solutions to mitigate the risk to a lower level.

| Risk ID | Event Description | Likelihood | Consequences | Overall Risk Rating | Priority |
|---------|---|------------|---------------|---------------------|----------|
| 1 | Access for undertaking work in Laboratory | Likely | Insignificant | M-6 | Moderate |
| 2 | Working with various materials for making specimens | Likely | Minor | H-5 | High |
| 3 | Handling heavy items / specimens | Likely | Major | E-3 | Extreme |
| 4 | Students understanding of using laboratory equipments for testing | Likely | Major | E-3 | Extreme |

| Risk ID | Event Description | Mitigation Strategy | Likelihood | Revision of Consequence | Overall Risk Rating |
|---------|--|---|------------|-------------------------|---------------------|
| 1 | Access for undertaking work in Laboratory | Plan suitable time with laboratory staff | Unlikely | L-8 | Low |
| 2 | Working with various materials for making specimens | Proper own PPE (i.e. gloves, safety boots, safety glasses etc) | Unlikely | L-7 | Low |
| 3 | Handling heavy items / specimens | Proper own PPE; seek for assistance if require | Unlikely | L-7 | Low |
| 4 | Students understanding of using laboratory equipment for testing | Student has previously been inducted and provide own PPE; seek for assistance if required | Unlikely | L-7 | Low |

Table 6: Risk methodology tables indicate the risks and solutions for mitigation

4. Experimental results and discussion

4.1 Failure mode

Failure of all test specimens was initiated with the development of hairline cracks. As the compressive load increased, the cracks were widened and propagated along the column. Local failure may have occurred to some of the specimens as cracks started to develop from the top of the columns. Spalling of the unconfined concrete cover was then observed, followed by buckling and rupturing of the longitudinal bars. The failure modes of the hollow concrete columns varied due to the different reinforcement ratio. There were evidenced ruptures to both the longitudinal bars and spirals, as well as damages to HCRS. Table 7 summarises the test concrete columns after failure.

Table 7 – Description of different failure mode of GFRP reinforced hollow concrete columns.

Specimen #2 “T”

1. Hairline cracks developed.
2. Cracks started at the top of column and propagated along the column
3. Spalling of overall concrete cover
4. Loud damage in the concrete core
5. Buckling in the longitudinal bars
6. GFRP bars, HCRS and concrete core slightly damage at the bottom of column



Specimen #2 “T” – 6 x 15.9mm dia. bars after failure

Specimen #4 “T”

1. Hairline cracks developed.
2. Cracks started at the top of column.
3. Spalling of overall concrete cover shortly after cracks developed.
4. Loud damage in the concrete core.
5. Slight buckle of the longitudinal bars.
6. Large damage of concrete core at the top of column.
7. Damage to the GFRP bars and HCRS at the top of column.



Specimen #4 “T” – 4 x 15.9mm dia. bars after failure

Specimen #5 “T”

1. Hairline cracks developed.
2. Cracks started at the top of column and propagated along column.
3. Spalling of overall concrete cover
4. Massive loud damage of the concrete core
5. Rupturing of GFRP spiral at the top of column
6. Rupturing and fibre splitting of five GFRP bars (out of a total eight bars) at the top of column.
7. Damage to HCRS at the top of column



Specimen #5 “T” – 8 x 15.9mm dia. bars after failure

Specimen #6 “C”

1. Hairline cracks developed.
2. Cracks started at the middle of column and propagated along column.
3. Spalling of overall concrete cover
4. Massive loud damage of the concrete core
5. Buckling in all the GFRP bars
6. Large crushing damage to the concrete core
7. Rupturing of GFRP bars and spiral at the top of column.



Specimen #6 “C” – 6 x 15.9mm dia. bars (no HCRS) after failure

Specimen #7 “C”

1. Hairline cracks developed.
2. Multiple cracks started simultaneously along column.
3. Spalling to majority of concrete cover.
4. Massive loud damage of the concrete core.
5. Buckling in the column.
6. Rupturing of GFRP spiral at the top of column.
7. Slight damage to HCRS.



Specimen #7 “C” – GFRP spirals and HCRS after failure

Specimen #8 “C”

1. Hairline cracks developed.
2. Multiple cracks started at the middle of the column.
3. Spalling to majority of concrete cover.
4. Multiple loud damages of the concrete core.
5. Buckling in the column.



Specimen #8 “C” – GFRP spirals after failure

4.2 Load-deformation behaviour

4.2.1 Load-deformation behaviour of Test columns

Figure 13 shows the axial load and deformation behaviour of the three test hollow concrete columns. Column #2 (6 x 15.9mm) initially had a brief non-linear ascending curve up to an axial load of 277.5kN and deformation of 3.75mm. Then a linear ascending slope reached the applied load of 1104kN (7.25mm deformation) before a slight non-linear ascending part due to cracks propagation. The first peak load resulted in 1397.1kN at 8.72mm. At this point, the unconfined concrete cover started to spall and a small load drop to 1341.8kN (4% drop) occurred. After spalling, the load was then carried by the confined concrete core, the longitudinal GFRP bars, lateral confinement by GFRP spirals and the HCRS. A linear ascending slope with many irregular load drops between 1st and 2nd peak loads. These load drops were due to buckling of longitudinal bars as well as crushing damage to concrete core. The 2nd peak load resulted in 1901.3kN at 16.17mm deformation before the column failed.

Column #4 (4 x 15.9mm) had a brief non-linear ascending curve up to 424.3kN at 7.57mm before a linear ascending slope reached 1159.9kN (11.16mm). Cracks started to propagate along the column height before it reached the 1st peak load of 1384.6kN at 13.03mm deformation. The concrete cover spalled at this point and a large load drop to 1160.9kN (16.2% drop) was noticed. This load drop of column #4 was greater than #2 due to the less reinforcement ratio of #4 (1.74% for #4 compare to 2.6% for #2). After the spalling, the ascending slope with a few load drops was observed until the 2nd peak load of 1598.7kN at 22.79mm deformation.

The load-deformation behaviour of column #5 was similar to that of #2, with their first peak axial load being close (1393.8kN for #2 and 1326.3kN at 9.92mm for #5). The second peak axial load of column #5 (2099.9kN at 22.15mm deformation) was 10.4% higher than specimen #2. Specimen #5 had a ductile failure behaviour that after the second peak load, a non-linear descending part for approximately 2mm deformation before failure.

Table 8 summarises the 1st and 2nd peak loads, deformations, bar strains, spiral strains, HCRS strains and concrete strains.

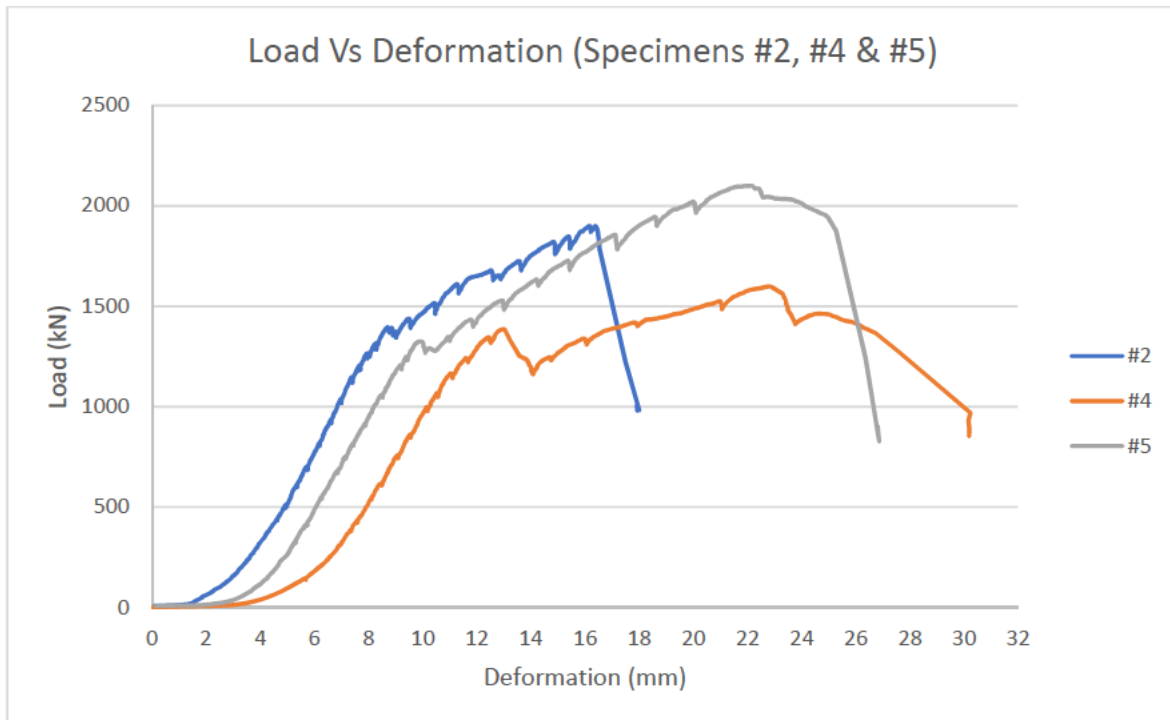


Figure 13 - Axial load and deformation behaviour of the Test concrete columns

| Specimen | 1st Peak Load (kN) | 2nd Peak Load (kN) | Confined Strength, fcc (MPa) | Deformation (yield), Δl (mm) | Deformation (ultimate), Δu (mm) |
|----------|--------------------|--------------------|------------------------------|------------------------------|---------------------------------|
| #2 | 1397.1 | 1901.3 | 49.7 | 8.72 | 16.17 |
| #4 | 1384.6 | 1598.7 | 49.3 | 13.03 | 22.79 |
| #5 | 1326.3 | 2099.9 | 47.2 | 9.92 | 22.15 |

| Specimen | Bar Strain at 1st Peak (μϵ) | Bar Strain at 2nd Peak (μϵ) | Spiral Strain at 1st Peak (μϵ) | Spiral Strain at 2nd Peak (μϵ) |
|----------|-----------------------------|-----------------------------|--------------------------------|--------------------------------|
| #2 | 2837 | 7977 | 1475 | 5695 |
| #4 | 1891 | 6590 | 775 | 2910 |
| #5 | 1861 | 7858 | 466 | 3741 |

| Specimen | HCRS Strain at 1st Peak (μϵ) | HCRS Strain at 2nd Peak (μϵ) | Concrete Strain at 1st Peak (μϵ) | Concrete Strain at 2nd Peak (μϵ) |
|----------|------------------------------|------------------------------|----------------------------------|----------------------------------|
| #2 | 375 | 625 | 1403 | 239 |
| #4 | 593 | 373 | 1536 | N/A |
| #5 | 420 | 243 | 420 | 243 |

Table 8 - Test results and sample details of the Test concrete columns
(Note: N/A indicates data not available)

4.2.2 Load-deformation behaviour of Controlled columns

Figure 14 shows the axial load and deformation behaviour of the three controlled hollow concrete columns. Similar to all the test columns, column #6 (6 x 15.9mm with no HCRS) initially had a brief non-linear ascending curve up to an axial load of 239.2kN and deformation of 5.84mm. It was followed by a linear ascending slope to applied load of 1091kN (9.34mm deformation) and cracks propagated afterwards. The first peak load reached 1312.8kN at 10.23mm. Spalling of overall column started at this point and a load drop to 1174.3kN (10.5% drop) occurred. After spalling, the axial load was carried by the concrete core and the longitudinal GFRP bars confined by the spirals. A non-linear ascending slope were caused by the crushing of concrete core as well as the buckling of GFRP bars. The 2nd peak load occurred when the load reached 1810.4kN and deformation of 32.16mm.

Column #7 (reinforced with spirals and HCRS) had a similar linear-elastic behaviour to #6. The first peak load resulted in 1309.8kN and 11.29mm deformation. A load drop to 1209.9kN (7.6% drop) occurred as a result of the partial spalling of concrete cover. The behaviour of column #7 at the plastic region (after 1st peak load) was different to #6 due to the omission of GFRP longitudinal bars. After spalling, lateral confinement of the spirals and HCRS were activated and only the concrete core was resisting the axial load. The 2nd peak load stopped at 24.1mm with a failure load of 1407.3kN.

Column #8 (reinforced with spirals only) had a distinctly different behaviour compared to all test and controlled columns due to the exclusion of the longitudinal bars and HCRS. A large deformation (22.6mm) at the start of the test as a result of the crushing of the non-reinforced column. The first peak load resulted in 1065.5kN (32.1mm deformation). Crushing of the concrete core was observed after the spalling and a brief increase to 1088.2kN (at 37.4mm) before the column failed.

Table 9 summarises the 1st and 2nd peak loads, deformations, bar strains, spiral strains, HCRS strains and concrete strains.



Figure 14 - Axial load and deformation behaviour of the Controlled concrete columns

| Specimen | 1st Peak Load (kN) | 2nd Peak Load (kN) | Confined Strength, f_{cc} (MPa) | Deformation (yield), Δl (mm) | Deformation (ultimate), Δu (mm) |
|----------|-----------------------|-----------------------|--------------------------------------|---|--|
| #6 | 1312.8 | 1810.4 | 46.7 | 10.23 | 32.16 |
| #7 | 1309.8 | 1407.3 | 46.6 | 11.29 | 24.1 |
| #8 | 1065.5 | 1088.2 | 37.9 | 32.13 | 37.4 |

| Specimen | Bar Strain at 1st Peak ($\mu\epsilon$) | Bar Strain at 2nd Peak ($\mu\epsilon$) | Spiral Strain at 1st Peak ($\mu\epsilon$) | Spiral Strain at 2nd Peak ($\mu\epsilon$) |
|----------|---|---|--|--|
| #6 | 1712 | 9807 | 619 | 5712 |
| #7 | N/A | N/A | 863 | 4501 |
| #8 | N/A | N/A | 624 | 3795 |

| Specimen | HCRS Strain at 1st Peak ($\mu\epsilon$) | HCRS Strain at 2nd Peak ($\mu\epsilon$) | Concrete Strain at 1st Peak ($\mu\epsilon$) | Concrete Strain at 2nd Peak ($\mu\epsilon$) |
|----------|--|--|--|--|
| #6 | N/A | N/A | 1494 | 309 |
| #7 | 537 | 364 | 1325 | 405 |
| #8 | N/A | N/A | 680 | 143 |

Table 9 - Test results and sample details of the Controlled concrete columns
(Note: N/A indicates data not available due to omission of reinforcement)

4.3 Strain behaviour of the GFRP bars and spirals

4.3.1 Strain behaviour of the GFRP bars and spirals for Test columns

Figure 15 shows the relationship between load and strains in the GFRP longitudinal bars (axial strains) and spirals (lateral strains) for all test columns. For the first peak load, the axial compressive strain recorded in the longitudinal bars was approximately $3000\mu\epsilon$ for column #2 and $2000\mu\epsilon$ for both #4 and #5. This was around 14.3% (#2) and 9.5% (#4 and #5) of the ultimate tensile strain of the GFRP reinforcement. Furthermore, the GFRP spirals recorded $1475\mu\epsilon$, $775\mu\epsilon$ and $466\mu\epsilon$ for columns #2, #4 and #5 respectively. These data representing all GFRP spirals were less than 7% of the ultimate tensile strength before the first peak load. Column #2 recorded a high axial strain of $2837\mu\epsilon$ at 1st peak load which indicated early concrete cracking, leading to early confinement by the GFRP spirals.

After the first peak load, the strain behaviour of the GFRP bars and spirals varied due to the different reinforcement ratio (ρ) of the column. With higher reinforcement ratio, columns #2 and #5, GFRP bars resisted higher axial loads compared to specimen #4 (Reinforcement ratio of #2, #4 and #5 were 2.6%, 1.74% and 3.47% respectively). Accordingly, #2 and #5 bars recorded failure strains of $7977\mu\epsilon$ and $7858\mu\epsilon$ in contrast to #4 $6590\mu\epsilon$. This indicated the failure strains of GFRP bars were less than 38% of the ultimate tensile strength.

Higher axial strain of columns #2 and #5 in GFRP bars also represented higher lateral strain in the spirals. At failure, the lateral strains were $5695\mu\epsilon$, $2910\mu\epsilon$ and $3741\mu\epsilon$ for #2, #4 and #5 respectively (lateral strains were less than 27% of the ultimate tensile strength). Therefore, it is concluded that by increasing the reinforcement ratio, it would increase the lateral contribution of the GFRP spirals at failure.

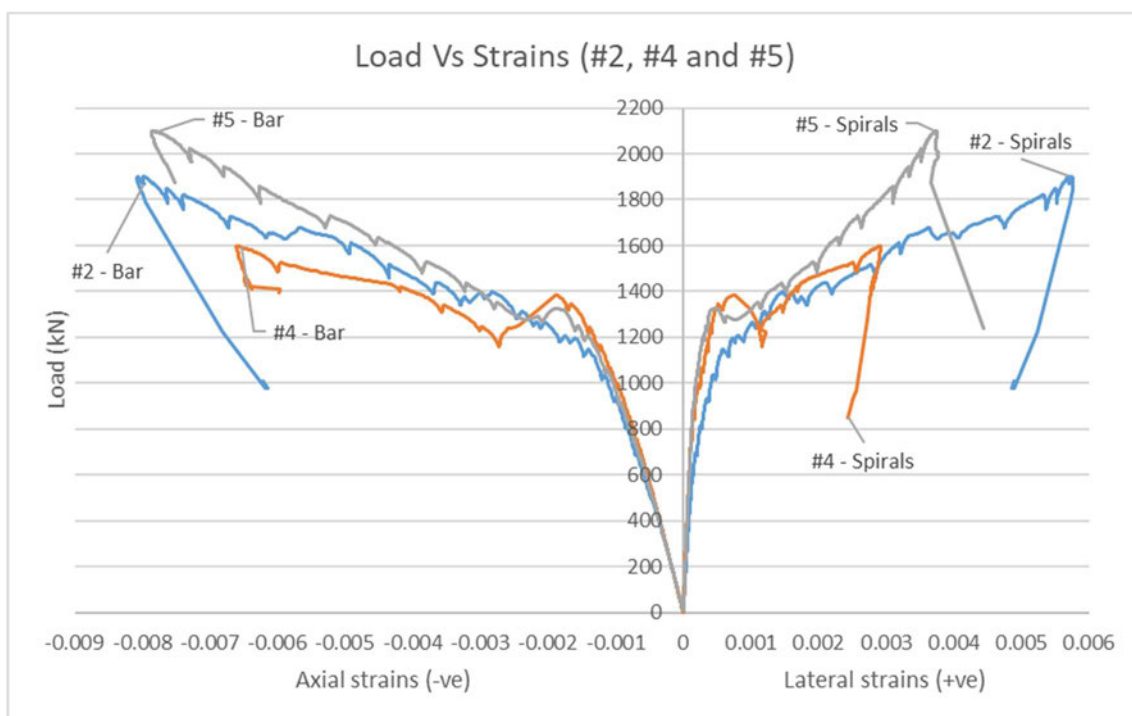


Figure 15 - Load and strain behaviour in longitudinal and transverse GFRP reinforcement (Test columns)

4.3.2 Strain behaviour of the GFRP bars and spirals for Controlled columns

Figure 16 shows the relationship between load and strains in the GFRP longitudinal bars (axial strains) and spirals (lateral strains) for all Controlled columns. The axial strain in #6 longitudinal bars at 1st peak was around $2000\mu\epsilon$, which was 9.5% of the ultimate tensile strain of the GFRP reinforcement. According to the Load-strain curve, the bars stopped resisting the axial loads from around $2000\mu\epsilon$ to $4000\mu\epsilon$ after spalling; therefore, only the concrete core resisted the loads. Axial strain of GFRP bars at $4000\mu\epsilon$ and lateral strain of spirals at $2000\mu\epsilon$ started resisting the loads after the crushing of concrete core. The column failed at axial strain of $9807\mu\epsilon$ and lateral strain of $5712\mu\epsilon$, 46.7% and 27.2% of the ultimate tensile strength respectively.

The lateral strains for columns #7 and #8 at 1st peak load was $862\mu\epsilon$ and $624\mu\epsilon$ respectively. Due to the omission of the longitudinal bars, #7 and #8 only relied on the concrete core to resist the axial loads. Both columns resulted at lateral strains of $4500\mu\epsilon$ (#7) and $3795\mu\epsilon$ (#8) at 2nd peak load.

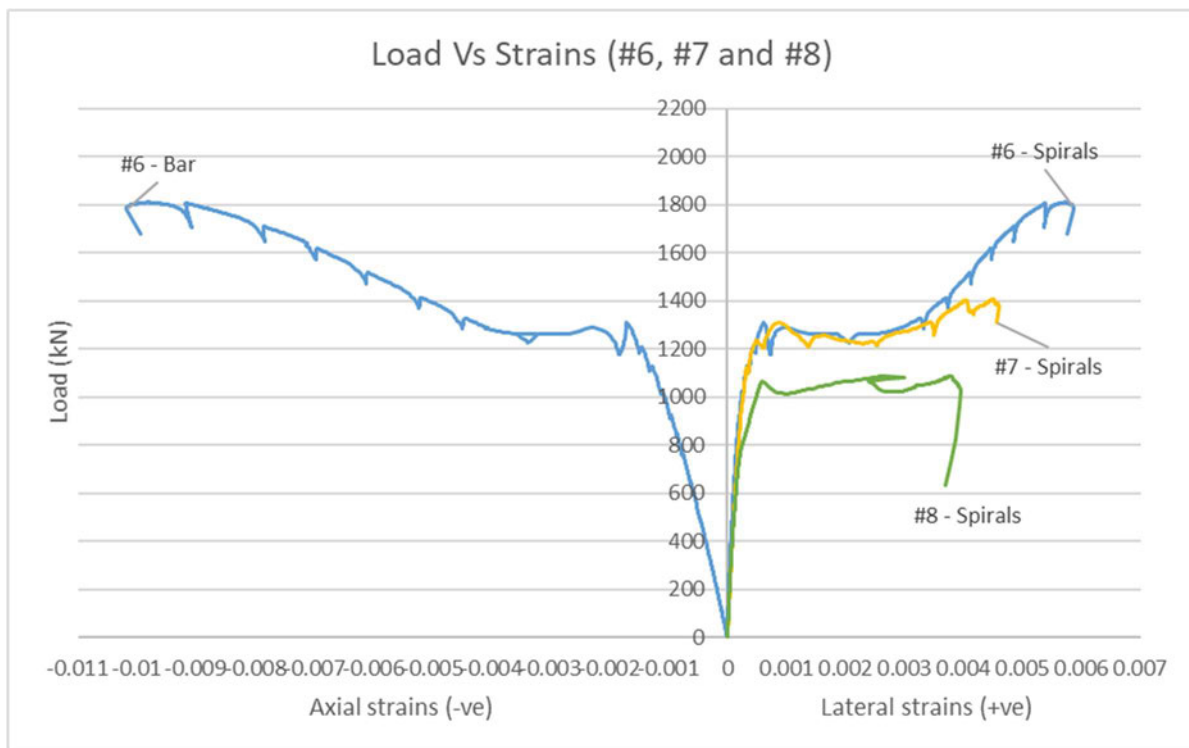


Figure 16 - Load and strain behaviour in longitudinal and transverse GFRP reinforcement (Controlled columns)

4.4 Strain behaviour of HCRS and the concrete

4.4.1 Strain behaviour of HCRS for all hollow concrete columns

Figure 17 shows the relationship between load and strains in the HCRS for all columns. All HCRS had a non-linear ascending behaviour until reaching the first peak load. However, the behaviour varied depending on the reinforcement ratio (ρ) after spalling. Columns #4 (4 x 15.9mm bars - $\rho = 1.74\%$) and #7 (no GFRP bars) had a lower ratio than #2 ($\rho = 2.6\%$) and #5 ($\rho = 3.47\%$). The concrete core of #4 and #7 contributed more axial load resistance and therefore HCRS mainly provided lateral confinement after the first peak load. On the other hand, the load contribution of GFRP bars was higher in columns #2 and #5 due to the increase in reinforcement ratio. It resulted in the HCRS provided more axial resistance as the applied load increased.

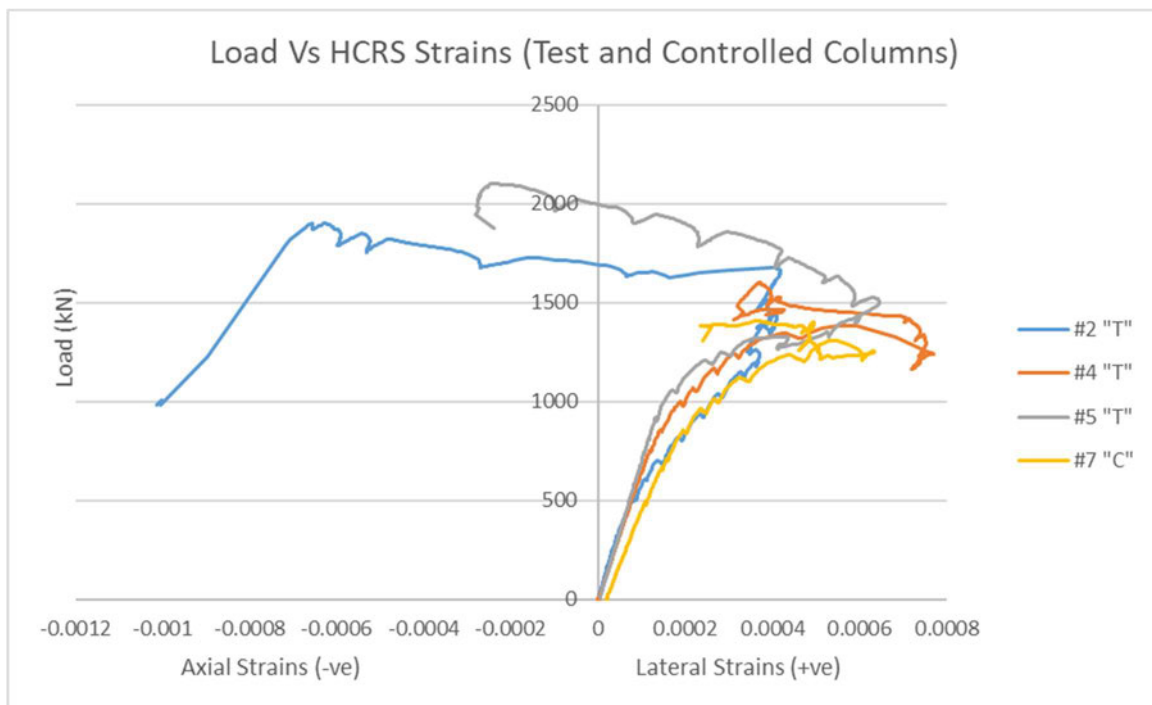


Figure 17 - Load and strain behaviour in HCRS (Test and Controlled columns)

4.4.2 Strain behaviour of the concrete for all hollow concrete columns

Figure 18 shows the relationship between load and strains in the concrete for all columns. An experimental error was made for column #5 and therefore the strain behaviour of concrete in #5 is excluded in this report.

In other columns, similar behaviour occurred before the 1st peak load. The axial strains in columns #2, #4, #6 and #7 measured around $1500\mu\epsilon$, with the exception of #8 measure at $1000\mu\epsilon$. These results responded to the strain at which the hairline cracks started to develop. However, the strain readings after the first peak load became unreliable and therefore should be omitted for this study.

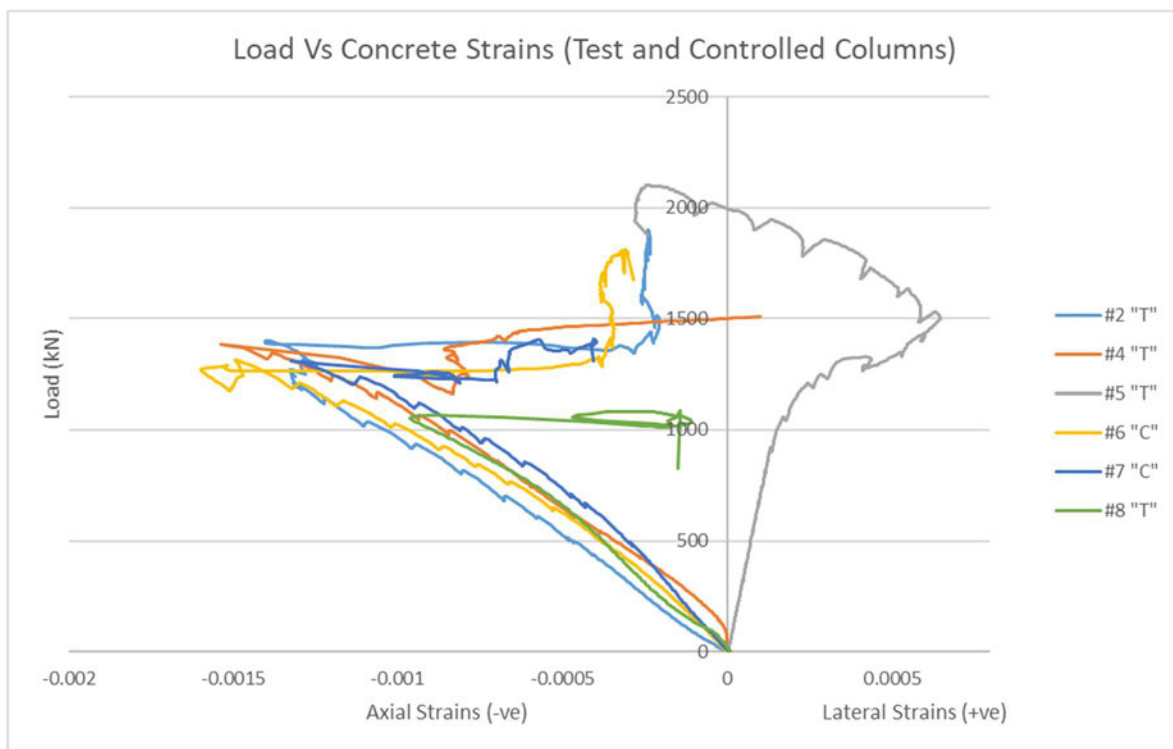


Figure 18 - Load and strain behaviour in the concrete (Test and Controlled columns)

4.5 Influence of the number of GFRP bars

Figure 13 shows the axial load and deformation behaviour of the test hollow columns with different reinforcement ratio with increasing the number of GFRP bars. Before the first peak load, the entire concrete area in column section was resisting the applied load. The first peak load of specimen #2, #4 and #5 were 1397.1kN, 1384.6kN and 1326.3kN respectively and only 5% difference between the maximum and minimum loads. It indicated that the reinforcement ratio at this stage did not affect the axial load capacity of the column as specimen #4 had a higher 1st peak load than #5. However, #4 experienced a higher load drop of 16.2% compared to #2 (4% drop) and #5 (4.6% drop) after concrete spalling. This can be explained that not only #2 and #5 had a higher reinforcement ratio, also by increasing the number of GFRP bars and it contributed a better reinforcement distribution to the column section. Therefore, lower reinforcement ratio and wide unconfined area between bars made column #4 more vulnerable to concrete cracking and crushing than its counterparts.

In the post loading stage, it was evident that different behaviour occurred between #2, #4 and #5. Column #4 had a lower reinforcement ratio; hence more applied load was resisted by the confined concrete core. This led to a non-linear behaviour of column #4. By contrast, #2 and #5 had a linear behaviour due to higher reinforcement ratio and more applied load was resisted by the longitudinal bars. Increasing the number of GFRP bars also contributed to the increase of the axial deformation capacity of the column. Accordingly, column #5 had a failure load of 2099.9kN, which was 10.4% higher than #2 (1901.3kN) and 31.4% higher than #4 (1598.7kN).

Furthermore, column #5 had a higher ductility than columns #2 and #4. Ductility is a physical property of a material's ability to undergo plastic deformation. It was measured with a ductility factor (μ) using Eq. 1 (Cui C, Sheikh; 2010) below.

$$\mu = \Delta u / \Delta l \quad (\text{Eq. 1})$$

where Δl – the deformation at 1st peak load
 Δu – the deformation at 2nd peak / failure load

Ductility factor (μ) was determined for each test column as follows.

$$\text{Column \#2 (6 x 15.9mm): } \mu = \Delta u / \Delta l = 16.17 / 8.72 = 1.85$$

$$\text{Column \#4 (4 x 15.9mm): } \mu = \Delta u / \Delta l = 22.79 / 13.03 = 1.71$$

$$\text{Column \#5 (8 x 15.9mm): } \mu = \Delta u / \Delta l = 22.16 / 9.92 = 2.23$$

Hence; column #2 to #5: $(2.23 - 1.85) / 1.85 = 20.5\%$; column #4 to #5: $(2.23 - 1.71) / 1.71 = 30.4\%$

As a result, column #5 had 20.5% and 30.4% higher ductility than columns #2 and #4 respectively. These findings highlight that increasing the reinforcement ratio would improve the structural properties of the hollow concrete columns.

4.6 Influence of HCRS

The hollow concrete columns #2 and #6 had the same number of GFRP bars (6 x 15.9mm) but different inner radial confinement. HCRS was installed in column #2 but not in #6. Figure 19 shows the axial load and deformation behaviour between these two columns. Both columns had initially had a brief non-linear ascending curve, with #6 deformed greater than #2 (6.1mm at 288.3kN for #6 compared to 4mm at 324.8kN for #2). A linear ascending slope then reached the first peak load for both #2 (1397.1kN at 8.7mm) and #6 (1312.8kN at 10.2mm). It represented an increase load capacity of 6.4% for column reinforced with HCRS at 1st peak stress. Column #2 experienced a load drop of 4% to 1341.8kN compared to 11.8% (1174.3kN) in #6 after concrete cover spalling due to early lateral confinement of HCRS.

The omission of HCRS caused a non-linear behaviour to column #6 after the first peak load as there was no radial confinement to the inner core of column. Figure 17 shows that HCRS provided both lateral and axial load capacity to #2. Therefore, column #2 had a failure load of 1901.3kN (at 16.2mm) which was 5% higher than #6 (1810.4kN at 32.2mm).

Initial observation on the load-deformation graph indicated that column #6 had a higher ductility than #2. However, the load and strain graph (figure 20) showed GFRP bars and spirals for column #6 stopped resisting the applied load from around $2000\mu\epsilon$ to $4000\mu\epsilon$. At this point, only the unconfined concrete core was resisting the loads and crushing of inner concrete wall occurred. This led to a non-ductile failure for column #6.

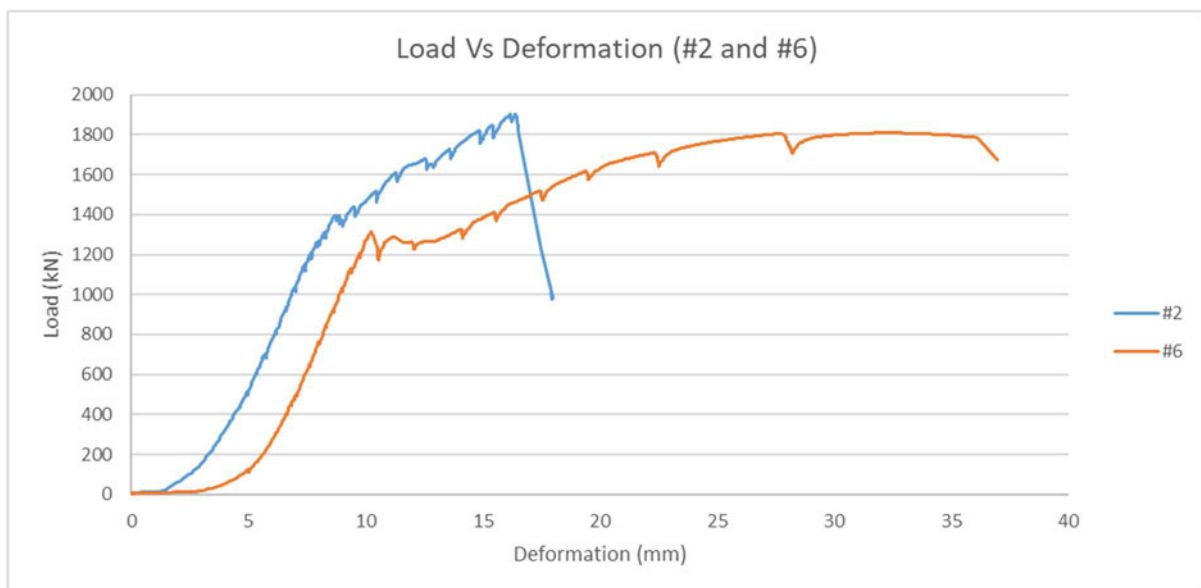


Figure 19 - Axial load and deformation behaviour of columns #2 and #6

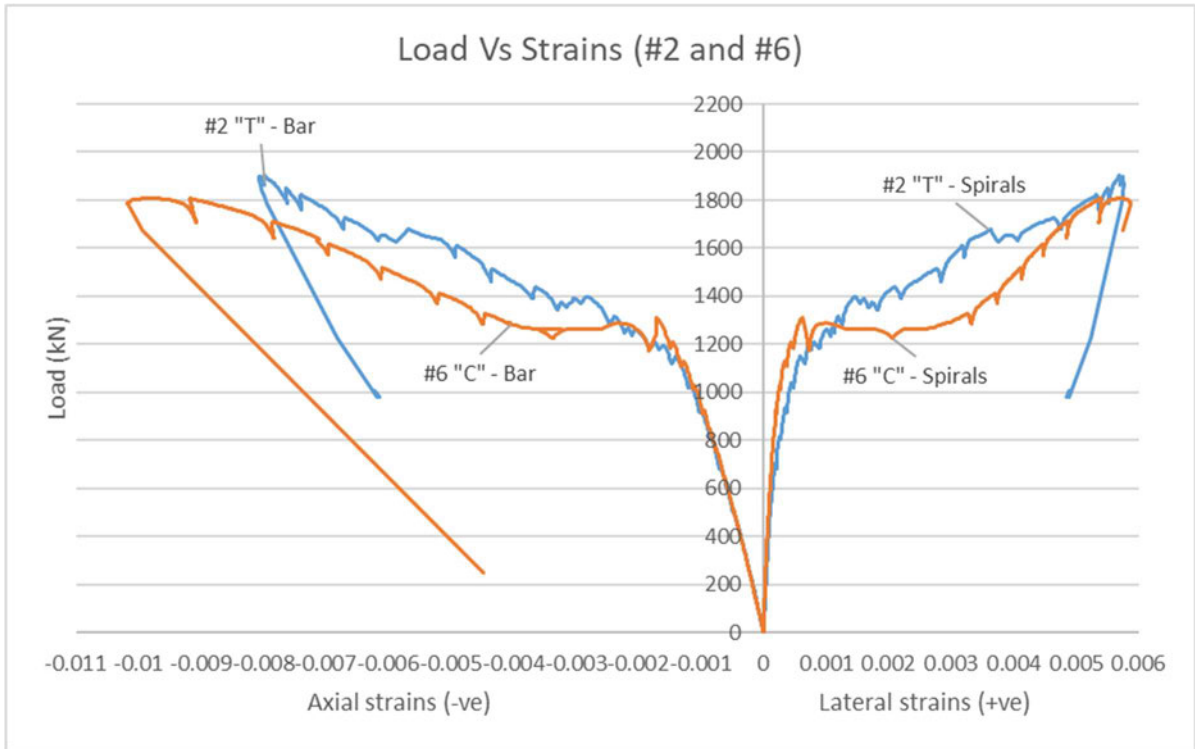


Figure 20 - Load and strain behaviour of columns #2 and #6

5. Theoretical analysis of column behaviour

5.1 Crushing strain and axial stress of the GFRP bars

The compressive behaviour of GFRP reinforcement is complex due to the nature of the material. GFRP rebar is made by pultrusion process with glass fibres impregnated in a thermosetting vinyl ester resin, additives and fillers. Therefore, GFRP is non-homogeneous and different failure modes such as global buckling or fibre micro-buckling may occur under compression. Previous study from Kobayashi and Fujisaki (1995) found that the compressive strength of glass fibre was approximately 30% of the tensile strength. However, Tobbi et al. (2014) have found the compressive behaviour of GFRP bars embedded in concrete was different to the behaviour of the bar by itself. The compressive behaviour of GFRP bars becomes linear-elastic when embedded in concrete, therefore the axial stress in GFRP bar can be found by using linear-elastic theory. This study also found the failure strain in compression of GFRP bars embedded in concrete was related the modulus of elasticity of GFRP bar (60.5GPa), the compressive strength of concrete and the lateral reinforcement.

Figure 21 indicates the relationship between the reinforcement ratio (ρ) to the stress contribution by GFRP bars at failure. AlAjarmeh et al (2019) found that the stress contribution can be calculated by multiplying the average strain of GFRP bars at failure by the modulus of elasticity of glass fibre reinforcement and the total area, then dividing it by the effective concrete core area confined by the transverse reinforcement. As a result, the stress contribution of the GFRP bars was directly proportional to the reinforcement ratio as shown in Eq. 2.

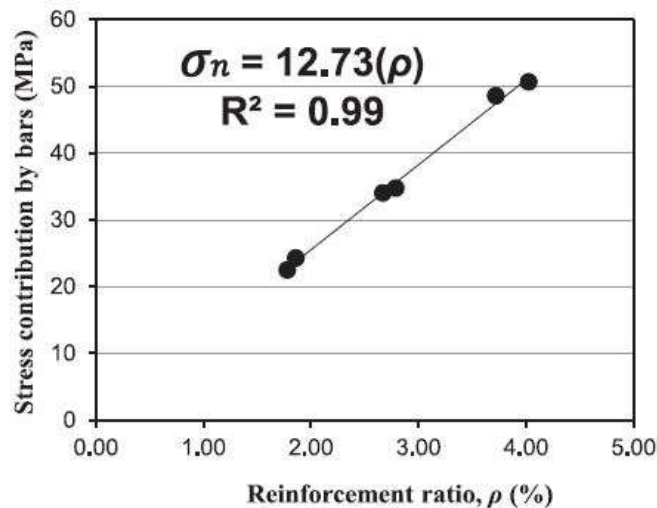


Figure 21 – Reinforcement ratio (ρ) Vs Stress contribution at failure

Stress contribution (σ_n) of GFRP bars,

$$\sigma_n = 12.73 \times \rho \quad (\text{Eq. 2})$$

$$\text{Specimen \#2} - 12.73 \times 2.6 = 33.1 \text{ MPa}$$

$$\text{Specimen \#4} - 12.73 \times 1.74 = 22.15 \text{ MPa}$$

$$\text{Specimen \#5} - 12.73 \times 3.47 = 44.17 \text{ MPa}$$

where reinforcement ratio, ρ :

$$\text{Specimen \#2} - 1191.3/45769 = 2.6\%$$

$$\text{Specimen \#4} - 794.2/45769 = 1.74\%$$

$$\text{Specimen \#5} - 1588.5/45769 = 3.47\%$$

The exact stress in GFRP bars at the failure can be calculated in Eq. 3 below.

Exact stress (σ_t) in GFRP bars at failure,

$$\sigma_t = \sigma_n \times A_{\text{core}} / A_{\text{GFRP}} \quad (\text{Eq. 3})$$

$$\text{Area of concrete core, } A_{\text{core}} = \pi D_o^2/4 - \pi D_i^2/4 = 28098 \text{ mm}^2$$

(where outside dia, $D_o = 200 \text{ mm}$, inside dia. $D_i = 65 \text{ mm}$)

Area of GFRP bars, A_{GFRP} :

$$\text{Specimen \#2} - 6 \times \pi \times 15.9^2 / 4 = 1191.3 \text{ mm}^2$$

$$\text{Specimen \#4} - 4 \times \pi \times 15.9^2 / 4 = 794.2 \text{ mm}^2$$

$$\text{Specimen \#5} - 8 \times \pi \times 15.9^2 / 4 = 1588.5 \text{ mm}^2$$

$$\sigma_t = \sigma_n \times A_{\text{core}} / A_{\text{GFRP}}$$

$$\text{Specimen \#2} - 33.1 \times 28098 / 1191.3 = 780.81 \text{ MPa}$$

$$\text{Specimen \#4} - 22.15 \times 28098 / 794.2 = 783.56 \text{ MPa}$$

$$\text{Specimen \#5} - 44.17 \times 28098 / 1588.5 = 781.46 \text{ MPa}$$

By using the linear elastic theory, the crushing strain can be determined from Eq. 4.

Crushing strain (ϵ_{cr}) of GFRP bars,

$$\epsilon_{\text{cr}} = \sigma_t / E_{\text{GFRP}} \quad (E_{\text{GFRP}} = 60.5 \text{ GPa}) \quad (\text{Eq. 4})$$

$$\text{Specimen \#2} - 780.81 / 60.5 \times 10^3 = 0.01291 \text{ (12906}\mu\epsilon\text{)}$$

$$\text{Specimen \#4} - 783.56 / 60.5 \times 10^3 = 0.01295 \text{ (12951}\mu\epsilon\text{)}$$

$$\text{Specimen \#5} - 781.46 / 60.5 \times 10^3 = 0.01292 \text{ (12917}\mu\epsilon\text{)}$$

According to Fillmore and Sadeghian (2018), the compressive strain of GFRP bars at failure is around 50% of the ultimate tensile strain (refer Table 3: Ultimate tensile strain of GFRP bars - $21,000\mu\epsilon$). The analytical results showed the crushing strains for specimens #2, #4 and #5 were 61.46%, 61.67% and 61.50% respectively. However, comparison between the analytical model to the experimental results in Table 10 indicated that the predicted failure strains for all test specimens were noticeably higher than the experimental one. This can be explained that the micro-buckling of the fibre in GFRP bars occurred prior to the failure of the hollow concrete column.

| Specimen | Gross area, A_g (mm^2) | Acore (mm^2) | ρ (%) | E_{GFRP} (Gpa) | Experimental Crushing Strain, $\mu\epsilon_{cr}$ | Analytical Crushing Strain, $\mu\epsilon_{cr,m}$ | $(\mu\epsilon_{cr,m}/\mu\epsilon_{cr}) * 100\%$ |
|----------|-------------------------------------|-------------------------|------------|-------------------------|--|--|---|
| #2 | 45769 | 28098 | 2.6 | 60.5 | 8071 | 12906 | 159.9 |
| #4 | 45769 | 28098 | 1.74 | 60.5 | 6609 | 12951 | 196.0 |
| #5 | 45769 | 28098 | 3.47 | 60.5 | 7864 | 12917 | 164.3 |

Table 10 – Comparison between experimental and analytical crushing strain of GFRP bars

5.2 Axial-load capacity (1st peak load)

From the beginning of the loading until reaching to the first peak load, the column demonstrated a linear elastic behaviour. This is because the entire concrete area in the section and the longitudinal reinforcements were resisting the applied load. During this phase, both the concrete and GFRP bars deformed at the same time. As a result, the first peak load capacity of GFRP reinforced concrete columns was calculated by its net area of the column, the contribution of the longitudinal reinforcement and the lateral confinement of the concrete core provided by HCRS.

In this study, the theoretical equation proposed by Hadi et al (2016) was adopted as it assumed the axial strain of GFRP bars was compatible with the ultimate axial strain of concrete at 0.003 (refer to Eq. 5). This correlated with experimental results as the axial compressive strain recorded in the GFRP bars ranged between 2000 $\mu\epsilon$ to 3000 $\mu\epsilon$ for specimens #2, #4 and #5.

Column load capacity, $P_n = P_{\text{concrete}} + P_{\text{GFRP bars}} + P_{\text{HCRS}}$

$$P_n = 0.85 \times f'_c \times (A_g - A_{\text{GFRP}}) + 0.003 \times E_{\text{GFRP}} \times A_{\text{GFRP}} + P_{\text{HCRS}} \quad (\text{Eq. 5})$$

Specimen #2:

$$0.85 \times 35 \times (45769 - 1191.3) + 0.003 \times 60.5 \times 10^3 \times 1191.3 + 84300 = 1326.2 + 216.2 + 84.3 \\ = \underline{1626.7\text{kN}}$$

Specimen #4:

$$0.85 \times 35 \times (45769 - 794.2) + 0.003 \times 60.5 \times 10^3 \times 794.2 + 84300 = 1338 + 144.1 + 84.3 \\ = \underline{1566.4\text{kN}}$$

Specimen #5:

$$0.85 \times 35 \times (45769 - 1588.5) + 0.003 \times 60.5 \times 10^3 \times 1588.5 + 84300 = 1314.4 + 288.3 + 84.3 \\ = \underline{1687\text{kN}}$$

Note:

P_{HCRS} was obtained from the experimental results at the first peak load of specimen #2 (6*15.9mm with HCRS) and specimen #6 (6*15.9mm no HCRS).

$$P_{\text{HCRS}} = 1397.1 (\#2) - 1312.8 (\#6) = 84.3\text{kN}$$

5.3 Axial-load capacity (2nd peak load)

After the first peak load, a total or partial spalling of the outer concrete cover occurred, which reduced the cross-section area of the column. At this stage, the applied load only resisted by the concrete core and the longitudinal reinforcement. The lateral reinforcements - GFRP spirals and HCRS activated after the first peak load to provide radial confinement to the concrete core.

In predicting the second axial-load capacity, the contribution of the concrete core and GFRP bars at the second peak load would be calculated. Similar to calculating the 1st peak load, the contribution of GFRP bars was determined by multiplying the crushing strain and the elastic modulus of the GFRP longitudinal reinforcement. Since the concrete core was subject to biaxial stress from 1st to 2nd peak load, the concrete contribution during this phase was based on the lateral confinement of the GFRP spirals.

AlAjarmeh et al. (2019) suggested that the lateral confinement, f_l (Figure 22) is based on the mechanical confinement concept but considers the void in hollow columns. Eq. 6 indicated lateral confinement was calculated by multiplying the cross-sectional area with the tensile strength and strain before failure of the GFRP spirals, then dividing it by the spacing of spiral and concrete core width. Since the GFRP spirals were only partially confining the concrete core, there were lateral damages of the unconfined concrete between the spacing of GFRP spirals. Therefore, the vertical spacing effect (Figure 23) was considered in calculating the confinement effectiveness ratio, k_e (Eq. 7). Furthermore, the opening effect between GFRP bars (Figure 24) was determined in finding the confinement effectiveness opening factor, k_o (Eq. 8).

It was suggested that the higher reinforcement ratio is, the higher degradation of the concrete core strength at the second peak load. This can be explained that high reinforcement ratio increased the effective axial stiffness of the GFRP bar's area, hence reduced the elastic modulus of the concrete at peak strength. The bar diameter factor, k_d (Eq. 9) was then calculated as a function of the normalised inertia moment between the bars and the concrete core (Figure 25). The effective lateral confinement, f_{le} (Eq. 10) was the product of bar diameter factor, k_d , the lateral confinement, f_l and the maximum between k_e and k_o (as the greater of k_e or k_o controlled partial damage). Referring to figure 26, the experimental concrete core strength, f_{ce} (Eq. 11) was taken as a function of the effective lateral confinement, f_{le} .

Finally, the predicted second peak load, P_{nt2} (Eq. 12) was the summation of the axial contribution from the longitudinal reinforcement (GFRP bars crushing strain, ϵ_{cr} (Eq. 4) x E_{GFRP} x A_{GFRP}), the contribution from the concrete core strength (f_{ce} x A_{cc}) and the confinement provided by HCRS. Furthermore, the maximum confined concrete strength, f_{ct} (Eq. 13) can be calculated by dividing the second peak load by the confined concrete core area. A comparison between experimental and analytical results of the second peak load is shown in Table 11. As discussed in Section 5.1, micro-buckling of the fibre in GFRP bars occurred prior to failure, therefore the experimental results of the second peak load were 5%, 11% and 7% lower than the analytical results for specimens #2, #4 and #5 respectively.

Although these analytical results were accurate for these test columns, further researches are necessary in order to provide a consolidated analytical model for hollow concrete columns reinforced with GFRP bars and HCRS.

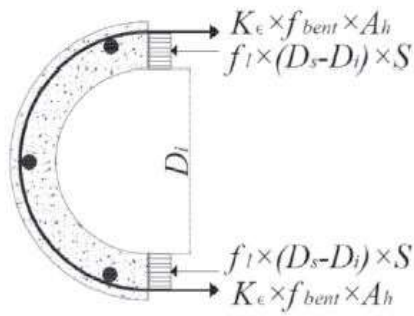


Figure 22 – Lateral confinement (f_l)

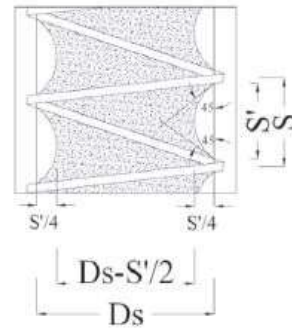


Figure 23 – Vertical spacing effect

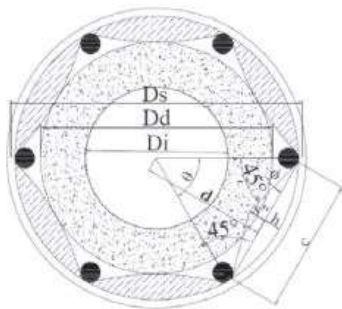


Figure 24 – Opening effect

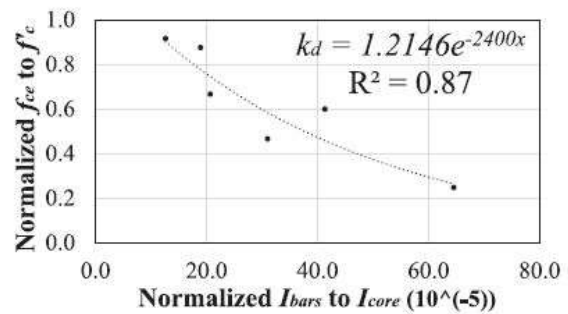


Figure 25 – Bar diameter factor, k_d

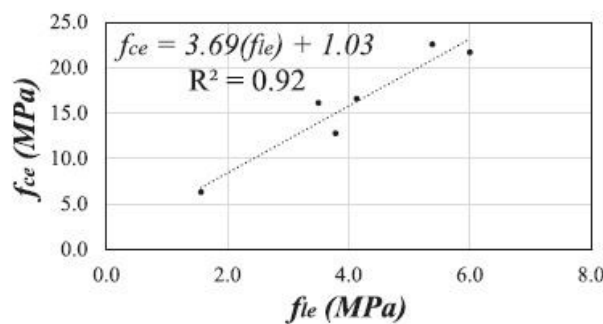


Figure 26 – Experimental concrete core strength, f_{ce}

Lateral confinement, f_l

$$f_l = 2A_h K_\epsilon f_{bent} / S (D_s - D_i) \quad (\text{Eq. 6})$$

where,

GFRP spiral (bar diameter, $d_b = 9.5\text{mm}$) cross-sectional area, A_h

$$A_h = \pi \times 9.5^2 / 4 = 70.88\text{mm}^2$$

GFRP ultimate tensile strength, $f_u = 1237.4\text{ MPa}$

GFRP spiral bent tensile strength, f_{bent} :

$$f_{bent} = (0.05 r/d_b + 0.3) f_u = 0.05 \times 98.5/9.5 + 0.3 \times 1237.4 = 1012.7\text{ MPa}$$

Spacing of spiral, $S = 50\text{mm}$;

Diameter of spiral, $D_s = 200\text{mm}$; Diameter of HCRS, $D_i = 65\text{mm}$

Area of concrete core, $A_{ce} = 28098\text{mm}^2$

Area of concrete core, A_{cc} (excluding GFRP bars)

$$\text{Specimen \#2: } A_{cc} = 28098 - 1191 = 26907\text{mm}^2$$

$$\text{Specimen \#4: } A_{cc} = 28098 - 794.2 = 27304\text{mm}^2$$

$$\text{Specimen \#5: } A_{cc} = 28098 - 1588 = 26510\text{mm}^2$$

$$f_l = 2A_h K_\epsilon f_{bent} / S (D_s - D_i) = 2 \times 70.88 \times 0.533 \times 1012.7 / 50 (200 - 65) = \underline{11.3\text{ MPa}}$$

Note: K_ϵ - the proportion of GFRP spiral ultimate strain before failure to ultimate tensile strength, taken as 0.533 (American Concrete Institute, 2015)

Confinement effectiveness ratio, k_e

$$k_e = A_{ce} / A_{cc} = \pi/4 [(D_s - S/4)^2 - D_i^2] / \pi/4 (D_s^2 - D_i^2) (1 - \rho) \quad (\text{Eq. 7})$$

$$\text{Specimen \#2: } k_e = [(200 - 50/4)^2 - 65^2] / (200^2 - 65^2) (1 - 0.026) = 0.887$$

$$\text{Specimen \#4: } k_e = [(200 - 50/4)^2 - 65^2] / (200^2 - 65^2) (1 - 0.0174) = 0.880$$

$$\text{Specimen \#5: } k_e = [(200 - 50/4)^2 - 65^2] / (200^2 - 65^2) (1 - 0.0347) = 0.896$$

Confinement effectiveness opening factor, k_o

$$k_o = A_d / A_{cc} = D_s^2 k_{of} - D_i^2 / (D_s^2 - D_i^2) (1 - \rho) \quad (\text{Eq. 8})$$

for k_{of} : #2, $\theta = 60^\circ$; #4, $\theta = 90^\circ$; #5, $\theta = 45^\circ$

$$\text{Specimen \#2: } k_{of} = [1/2 + (\cos 60/2)/2 - (\sin 60/2 \tan(45 - 60/2)/4)]^2 = 0.81$$

$$K_o = 200^2 \times 0.81 - 65^2 / (200^2 - 65^2) (1 - 0.026) = 0.81$$

$$\text{Specimen \#4: } k_{of} = [1/2 + (\cos 90/2)/2 - (\sin 90/2 \tan(45 - 90/2)/4)]^2 = 0.73$$

$$K_o = 200^2 \times 0.73 - 65^2 / (200^2 - 65^2) (1 - 0.0174) = 0.71$$

$$\text{Specimen \#5: } k_{of} = [1/2 + (\cos 45/2)/2 - (\sin 45/2 \tan(45 - 45/2)/4)]^2 = 0.85$$

$$K_o = 200^2 \times 0.85 - 65^2 / (200^2 - 65^2) (1 - 0.0347) = 0.86$$

Bar diameter factor, kd

$$kd = 1.215 \times e^{-2400 \times I_{\text{bars}} / I_{\text{core}}} \quad (\text{Eq. 9})$$

$$I_{\text{core}} = D^4/64 - d^4/64 = \pi \times 250^4/64 - \pi \times 65^4/64 = 191 \times 10^6 \text{ mm}^4$$

Specimen #2:

$$I_{\text{bars}} = 6 \times \pi d_b^4/64 = 18822 \text{ mm}^4$$

$$kd = 1.215 \times e^{-2400 \times 18822 / 191 \times 10^6} = 0.959$$

Specimen #4:

$$I_{\text{bars}} = 4 \times \pi d_b^4/64 = 12549 \text{ mm}^4$$

$$kd = 1.215 \times e^{-2400 \times 12549 / 191 \times 10^6} = 1.038$$

Specimen #5:

$$I_{\text{bars}} = 4 \times \pi d_b^4/64 = 25096 \text{ mm}^4$$

$$kd = 1.215 \times e^{-2400 \times 25096 / 191 \times 10^6} = 0.886$$

Effective lateral confinement, fle

$$fle = \text{Max}(k_e, k_o) \times kd \times f_l \quad (\text{Eq. 10})$$

(Note: k_e is greater than k_o in all specimens)

$$\text{Specimen \#2: } fle = 0.887 \times 0.959 \times 11.3 = \underline{9.61 \text{ MPa}}$$

$$\text{Specimen \#4: } fle = 0.880 \times 1.038 \times 11.3 = \underline{10.32 \text{ MPa}}$$

$$\text{Specimen \#5: } fle = 0.896 \times 0.886 \times 11.3 = \underline{8.97 \text{ MPa}}$$

Experimental concrete core strength, fce

$$fce = 3.69 fle + 1.03 \quad (\text{Eq. 11})$$

$$\text{Specimen \#2: } fce = 3.69 \times 9.61 + 1.03 = \underline{36.49 \text{ MPa}}$$

$$\text{Specimen \#4: } fce = 3.69 \times 10.32 + 1.03 = \underline{39.11 \text{ MPa}}$$

$$\text{Specimen \#5: } fce = 3.69 \times 8.97 + 1.03 = \underline{34.13 \text{ MPa}}$$

Predicted second (2nd) peak load, Pnt2

$$Pnt2 = fce Acc + P_{HCRS (Pnt2)} + \epsilon_{cr} E_{GFRP} A_{GFRP} \quad (Eq. 12)$$

Specimen #2: $Pnt2 = 36.49 \times 26907 + 90.9 \times 10^3 + 0.01291 \times 60.5 \times 10^3 \times 1191 = \underline{2002.3 \text{ kN}}$

Specimen #4: $Pnt2 = 39.11 \times 27304 + 90.9 \times 10^3 + 0.01295 \times 60.5 \times 10^3 \times 794.2 = \underline{1781 \text{ kN}}$

Specimen #5: $Pnt2 = 34.13 \times 26510 + 90.9 \times 10^3 + 0.01292 \times 60.5 \times 10^3 \times 1588 = \underline{2237 \text{ kN}}$

Note:

$P_{HCRS (Pnt2)}$ was obtained from the experimental results at the 2nd peak load of specimen #2 (6*15.9mm with HCRS) and specimen #6 (6*15.9mm no HCRS).

$$P_{HCRS (Pnt2)} = 1901.3 (\#2) - 1810.4 (\#6) = 90.9\text{kN}$$

Maximum confined concrete strength, fcct

$$fcct = Pnt2 / A_{core} \quad (Eq. 13)$$

Specimen #2: $fcct = 1181.6 \times 10^3 / 28098 = \underline{42.05 \text{ MPa}}$

Specimen #4: $fcct = 895.3 \times 10^3 / 28098 = \underline{31.86 \text{ MPa}}$

Specimen #2: $fcct = 1475.1 \times 10^3 / 28098 = \underline{52.5 \text{ MPa}}$

| Specimen | ke | ko | kd | fle (MPa) | fce (MPa) | Pnt2 (kN) | fcct (MPa) | Pn2 (kN) | Pnt2 / Pn2 |
|----------|-------|------|-------|--------------|--------------|--------------|---------------|-------------|------------|
| #2 | 0.887 | 0.81 | 0.959 | 9.61 | 36.49 | 2002.3 | 42.05 | 1901.3 | 1.05 |
| #4 | 0.880 | 0.71 | 1.038 | 10.32 | 39.11 | 1781 | 31.86 | 1598.7 | 1.11 |
| #5 | 0.896 | 0.86 | 0.886 | 8.97 | 34.13 | 2237 | 52.5 | 2099.9 | 1.07 |

Table 11 – Comparison between experimental and analytical results

6. Conclusions

The objective of this study was to investigate the effect of reinforcement ratios on the axial compression behaviour of hollow concrete columns by increasing the number of longitudinal GFRP bars. This research was aimed at determining the compressive capacity, reinforcement displacement and failure modes of the concrete specimens. Based on the experimental test results and analytical modelling in this study, the following conclusions can be drawn.

1. The reinforcement ratio affected the axial load deformation behaviour of the hollow concrete columns. Increasing the reinforcement ratio enhanced the axial load capacity of the RC columns. By increasing 4 pieces of 15.9mm diameter bars to 8 pieces, the axial compressive strength increased by 31.4%.
2. Using more longitudinal GFRP bars enhanced the ductility of the hollow concrete columns. Ductility factor of the RC columns increased by 30.4% when the longitudinal reinforcement increased from 4 to 8 pieces of 15.9mm diameter GFRP bars.
3. High reinforcement ratio reduced the load drop after the first peak load. The load drop for 4*15mm dia. column was 16.2%, which was significantly greater than other specimens as the load drops for 6*15.9mm dia. and 8*15.9mm dia. were 2.1% and 4.6% respectively.
4. Close GFRP spiral spacing increased the compressive strength in the longitudinal bars. Analytical modelling showed that the average exact stress in GFRP bars at failure was 782MPa. Previous study from Tobbi et al. (2012) suggested the compressive strength of GFRP bar was around 30% to 40% of its tensile counterpart (Note: refer to Table 3 - ultimate tensile strength of GFRP bar is 1237.4MPa, hence compressive strength is approximately 430MPa). The close spiral spacing of 50mm enhanced the lateral confinement of the column and resulted in improving the compressive strength of GFRP bars embedded in concrete.
5. Omission of HCRS in hollow concrete column changed the failure mode from ductile to non-ductile. Load-strain graph of column #2 and #6 (Figure 20) indicated that without HCRS, crushing of concrete inner wall occurred for column #6, leading to a non-ductile failure.
6. Fillmore and Sadeghian (2018) found that the compressive strain of GFRP bars at failure was around 50% of the ultimate tensile strain. In this study, the average crushing strain for test columns was relatively low at 35.8%. Since the failure strain in compression of GFRP bars embedded in concrete is closely related to the concrete compressive strength, higher concrete grade may be used in future researches to improve the compressive strain of GFRP bars.
7. In order to determine the ultimate load capacity of the hollow concrete columns, measures must be taken to control local failure in future studies.

7. References:

1. AlAjarmeh, O.S.; Manalo, A.; Benmokrane, B.; Karunasena, W.; Mendis, P.; 2019. Axial performance of hollow concrete columns reinforced with GFRP composite with different reinforcement ratios. – Elsevier Composite Structures
2. AlAjarmeh, O.S.; Manalo, A.C.; Benmokrane, B.; Karunasena, W.; Mendis, P.; Nguyen, K.T.Q.; 2019. Compressive behaviour of axially loaded circular hollow concrete columns reinforced with GFRP bars and spirals – Construction and Building Materials
3. Afifi, M.Z.; Mohamed, H.M.; Benmokrane, B.; 2013. Axial capacity of circular concrete columns reinforced with GFRP bars and spirals – American Society of Civil Engineers
4. Tobbi, H.; Farghaly, A.S.; Benmokrane, B.; 2014. Behavior of concentrically loaded fiber-reinforced polymer reinforced concrete columns with varying reinforcement type and ratios – ACI Structural Journal Technical Paper
5. Karim, H.; Sheikh, M.N.; Hadi, M.N.S.; 2016. Axial load-axial deformation behaviour of circular concrete columns reinforced with GFRP bars and helices – University of Wollongong
6. Pantelides, C.P.; Gibbons, M.E.; Reaveley, L.D.; 2013. Axial load behaviour of concrete columns confined with GFRP spirals – Journal of Composites for Construction
7. Becque J.; Patnaik, A.K.; Rizkalla, S.H.; 2003. Analytical models for concrete confined with FRP tubes – Journal of Composites for Construction
8. Hadi, M.N.; Wany, W.; Sheikh, M.N.; 2015. Axial compressive behaviour of GFRP tube reinforced concrete columns – University of Wollongong
9. Maranan, G.B.; Manalo, A.C.; Benmokrane, B.; Karunasena, W.; Mendis, P.; 2016. Behavior of concentrically loaded geopolymer-concrete circular columns reinforced longitudinally and transversely with FGRP bars – Elsevier Engineering Structures
10. De Luca, A.; Matta, F.; Nanni, A.; 2010. Behavior of full-scale glass fiber-reinforced polymer reinforced concrete columns under axial load – ACI Structural Journal Technical Paper
11. Mohamed, H.M.; Afifi, M.Z.; Benmokrane, B.; 2014. Performance evaluation of concrete columns reinforced longitudinally with FRP bars and confined FRP hoops and spirals under axial load – American Society of Civil Engineers.
12. Tobbi, H.; Farghaly, A.; Benmokrane, B.; 2012. Concrete columns reinforced longitudinally and transversally with glass fibre-reinforced polymer bars. ACI Structural Journal Technical Paper (Title no. 109-S48)
13. Cui C, Sheikh S; Experimental study of normal and high strength concrete confined with fiber-reinforced polymers – ASCE J Compos Constr; 2010; 14:533-61
14. Fillmore B, Sadeghian P; Contribution of longitudinal GFRP bars in concrete cylinders under axial compression. Can J Civ Eng 2018; 45(6): 458-68.
15. ACI; Guide for the design and construction of concrete reinforced with FRP bars; Farmington Hills, MI: American Concrete Institute; 2015.

Appendix A: Project Specification

ENG4111 & ENG4112 Research Project

Project Specification

For: Michael Ng

Title: The Effect of Number of Glass Fibre Reinforced Polymer (GFRP) bars on the Behaviour of Concrete Columns with Hollow Composite Reinforcing System (HCRS)

Major: Civil Engineering

Supervisors: Dr. Allan Manalo; Omar Alajarmeh

Enrolment: ENG4111 – EXT S1, 2019; ENG4112 – EXT S2, 2019

Project Aim: To investigate the compressive behaviour and evaluate the strength and strain capacities of concrete column reinforced with GFRP bars with ligatures and HCRS. This project focuses on the failure mode of the concrete columns with laboratory testing and theoretical analysis using different reinforcement materials, by which the advantages/disadvantages of using GFRP bars and HCRS will be identified as a means of reinforcement in concrete columns.

Programme: Version 1, 21st March 2019

1. Research the background information relating to hollow concrete columns reinforced with GFRP bars and HCRS.
2. Theoretical evaluation and prediction of failure load for hollow concrete columns reinforced with GFRP bars and HCRS.
3. Review relevant standards for design procedures of RC columns for their strength and serviceability.
4. Review the procedures for concrete testing in the laboratory and liaise with USQ Professional Staff in relation to producing the specimens for testing.
5. Investigate by experimental testing the effect of reinforcement ratio by increase the number of GFRP bars.
6. Critical analyses and interpretation of test results, and comparison theoretical prediction.
7. Make recommendations on the use of GFRP bars and HCRS.
8. Submit final dissertation on research, theoretical analysis, testing, results and conclusion.

If time permits:

- To develop a simplified theoretical model that will explain the behaviour of hollow concrete columns reinforced with HCRS and GFRP bars of different number of bars.

Appendix B: Project Plan

